Supporting Information for:

Proton-Induced Reactivity of NO^- from a $\{CoNO\}^8$ Complex

Melody A. Rhine,[†] Andria V. Rodrigues,[‡] Ramona J. Bieber Urbauer,[†] Jeffrey L. Urbauer,[†] Timothy L. Stemmler,[‡] and Todd C. Harrop[*,†]

[†]Department of Chemistry and Center for Metalloenzyme Studies, The University of Georgia, 1001 Cedar Street, Athens, Georgia 30602, United States

[‡]Departments of Pharmaceutical Sciences, Biochemistry and Molecular Biology, Wayne State University, Detroit, Michigan 48201, United States

*E-mail: tharrop@uga.edu

Table of Contents:

Experimental

General Information. All reagents were purchased from commercial suppliers and used as received unless otherwise noted. Research grade nitric oxide gas (NO(g), UHP, 99.5%) was obtained from Matheson Tri-Gas. The NO(g) was purified by passage through an Ascarite II® (sodium hydroxide-coated silica, purchased from Aldrich) column and handled under anaerobic conditions. ^{15}NO(g) (^{15}N ≥ 98%) was procured from Cambridge Isotope Labs and used as received. Acetonitrile (MeCN), tetrahydrofuran (THF), dichloromethane (CH_2Cl_2), and diethyl ether (Et_2O) were purified by passage through activated alumina columns using an MBraun MB-SPS solvent purification system and stored over 3 Å molecular sieves under an N_2 atmosphere before use. Anhydrous 2-methyltetrahydrofuran (2-MeTHF) was obtained by storage over 3 Å molecular sieves for 48 h, decanting from the sieves, and storage under N_2. The Co(II) salt $(Et_4N)_2[CoCl_4]$ was prepared according to the published procedure.[1] The N_4-ligand (*N*^{1}*E*,*N*^{2}*E*)-*N*^{1},*N*^{2}-bis((1H-pyrrol-2-yl)methylene)-4,5-dichlorobenzene-1,2-diamine (abbreviated as $LN_4H_2^{PhCl}$, where H = dissociable protons) was synthesized according to the published procedure.[2] The $\{Co(NO)_2\}^{10}$ synthon, $[Co_2(\mu\text{-}Cl)_2(NO)_4]$, was also synthesized according to the published procedure.[3] All reactions were performed under an inert atmosphere of N_2 using standard Schlenk techniques or in an MBraun Unilab glovebox under an atmosphere of purified N_2. Reactions involving NO(g) and nitroxyl transfer were performed with minimal light exposure by wrapping the reaction flasks/vials with aluminum foil to avoid any photochemical reactions.

Physical Methods. FTIR spectra were collected with a ThermoNicolet 6700 spectrophotometer running the OMNIC software. Solid-state samples were prepared as KBr pellets, while solution-state spectra were obtained using a demountable airtight liquid IR cell from Graseby-Specac with CaF_2 windows and 0.1 mm PTFE spacers. All FTIR samples were prepared inside a glovebox under an inert atmosphere of purified N_2. The closed liquid cell was taken out of the box and spectra were acquired immediately. X-band (9.60 GHz) EPR spectra were obtained using a Bruker ESP 300E EPR spectrometer controlled with a Bruker microwave bridge at 10 K. The EPR was equipped with a continuous-flow liquid He cryostat and a temperature controller (ESR 9) made by Oxford Instruments Inc. Electronic absorption spectra were performed at 298 or 310 K using a Cary-50 UV-vis spectrophotometer containing a Quantum Northwest TC 125 temperature control unit. The UV-vis samples were prepared anaerobically in gas-tight Teflon-lined screw cap quartz cells with an optical pathlength of 1 cm. Electrochemistry measurements were performed with a PAR Model 273A potentiostat using a non-aqueous Ag/Ag^+ (0.01 M $AgNO_3$/0.1 M ^{n}Bu$_4$NPF$_6$ in CH_3CN) reference electrode, Pt-wire counter electrode, and a Glassy Carbon working milli-electrode (diameter = 2 mm) under an Ar atmosphere. Measurements were performed at ambient temperature using 1.0-10.0 mM analyte in THF containing 0.1 M ^{n}Bu$_4$NPF$_6$ as the supporting electrolyte. Ferrocene (Fc) was used as an internal standard and all potentials are reported relative to the Fc^+/Fc couple ($E_{½}$ = 0.258 V in THF versus the prepared Ag/Ag^+ reference electrode). ^{1}H, ^{15}N, and ^{31}P NMR spectra were recorded in the listed deuterated solvent with a 400 MHz Bruker BZH 400/52 NMR spectrometer or a Varian Unity Inova 500 MHz NMR spectrometer at 298 K with chemical shifts internally referenced to tetramethylsilane (TMS = $Si(CH_3)_4$), CH_3NO_2, 85% H_3PO_4 (external), respectively, or the residual protio signal of the deuterated solvent as previously reported.[4] The identification of P-containing molecules was verified by comparison to commercially-available standards or literature values. Under our conditions, the ^{31}P chemical shift of Ph_3P and Ph_3P=O is -6.0 and

26.3 ppm, respectively ($(CD_3)_2SO$ vs. external 85% H_3PO_4). The reported ^{31}P chemical shift for $Ph_3P{=}NH$ is 35.45 ppm in $(CD_3)_2SO$,[5] which was confirmed by an independent synthesis of this material. However, this value is for the protonated salt $Ph_3P{=}NH{\bullet}H_2SO_4$. Attempts to generate the free base $Ph_3P{=}NH$ resulted in $Ph_3P{=}O$ due to the unstable nature of the ylide. The reported ^{31}P value for $Ph_3P{=}NH$ in the solid-state is 21.8 ppm, whereas the protonated salt $Ph_3P{=}NH{\bullet}HBr$ is 34.8 ppm.[6] The former value is consistent with our value of 20.6 ppm. This value also trends with those obtained by King for in situ formation of $Ph_3P{=}NH$ in D_2O.[5b] Low resolution ESI-MS data were collected on a Bruker Esquire 3000 plus ion trap mass spectrometer. High resolution ESI-MS data were collected using an Orbitrap Elite system with CID for MS-MS with precision to the third decimal place. Elemental microanalyses for C, H, and N were performed by Columbia Analytical Services (Tucson, AZ) or QTI-Intertek (Whitehouse, NJ). HPLC was conducted for separation and analysis using a Waters 2487 HPLC with a Waters 600 Controller and dual λ absorbance detector monitoring at 212 nm and 228 nm. Separations were performed on a Phenomenex Luna® reverse phase C18 (250 × 4.6 mm/10 μm) column, 10 μm particle size, 200 μL loop volume with 150 μL loop injections (flow rate: 1 mL/min), and effected by means of an isocratic MeCN/H_2O (65/35) gradient for separating Ph_3P and $Ph_3P{=}O$.[7]

Synthesis of Compounds:

$[Co(LN_4^{PhCl})(NO)]$, $\{CoNO\}^8$ (1). To a 2 mL MeCN slurry of red-brown $LN_4H_2^{PhCl}$ (300.0 mg, 0.9058 mmol) was added a 2 mL MeCN slurry of NaH (48.9 mg, 2.04 mmol) resulting in a yellow-brown solution and H_2(g) evolution. This solution was stirred at RT for 30 min during which time an occasional vacuum was introduced to remove H_2(g). After this time, a 5 mL blue slurry of $(Et_4N)_2[CoCl_4]$ (417.8 mg, 0.9058 mmol) in MeCN was added causing an instantaneous color change to deep red-brown indicative of complex formation. A small amount of light gray solid was also observed in the reaction mixture (NaCl). The reaction mixture stirred at 60 °C with a H_2O bath for 3 h that resulted in no further change. The solution was then cooled to RT, filtered, and the NaCl solid washed with 2 mL of cold MeCN. The red-brown MeCN filtrate containing $(Et_4N)_2[Co(LN_4^{PhCl})Cl_2]$ was next purged with a stream of NO(g) for 1.5 min at 60 °C. Addition of NO(g) resulted in an immediate albeit slight color change; the solution became darker brown (red-tinted) and a dark microcrystalline precipitate was immediately observed. The reaction mixture stirred at 60 °C for 30 min under an NO atmosphere in the headspace of the flask. After this time, the solution was cooled to RT and excess NO(g) was removed by pulling vacuum and refilling with N_2. The reaction mixture was then placed in a -24 °C freezer for 2 h to induce further precipitation. The resulting microcrystalline solid was filtered, washed with 3 mL of MeCN, and dried under vacuum to afford 272.7 mg (0.6522 mmol, 72%) of product. FTIR (KBr matrix), ν_{max} (cm^{-1}): 3091 (w), 1667 (s, ν_{NO}), 1568 (s), 1541 (s), 1522 (s), 1501 (s), 1453 (m), 1435 (w), 1379 (s), 1328 (w), 1291 (s), 1271 (s), 1256 (s), 1195 (m), 1118 (m), 1037 (s), 984 (m), 913 (m), 882 (w), 855 (m), 827 (w), 810 (w), 753 (s), 680 (w), 663 (w), 602 (w), 529 (w), 472 (w), 432 (w). Solution FTIR (CaF_2 windows, 0.1 mm spacers, RT, cm^{-1}): ν_{NO} = 1670 (THF), 1679 (CH_2Cl_2). UV-vis (THF, 298 K), λ_{max}, nm (ε, $M^{-1}\,cm^{-1}$): 326 (14,000), 368 (18,000), 464 (9,300), 505 (sh 7,500). ^1H NMR (500 MHz, THF-d_8, δ from residual protio solvent): 8.14 (s, 1H), 7.78 (d, 1H, J = 2.0 Hz), 7.56 (s, 1H), 7.06 (br m, 1H), 6.37 (br m, 1H). Anal. Calcd. for $C_{16}H_{10}Cl_2CoN_5O$: C, 45.96; H, 2.41; N, 16.75. Found: C, 45.97; H, 2.68; N, 16.11.

[Co(LN$_4$^{PhCl})(^{15}NO)], {Co^{15}NO}^{8} (1-^{15}NO). The isotopically-labeled complex **1-^{15}NO** was prepared analogously to **1** except for using 200.0 mg (0.6039 mmol) of LN$_4$H$_2$^{PhCl}, 278.6 mg (0.6040 mmol) of $(Et_4N)_2[CoCl_4]$, and 32.6 mg (1.36 mmol) of NaH to generate $(Et_4N)_2$[Co(LN$_4$H$_2$^{PhCl})Cl$_2$] *in situ* followed by purging of ^{15}NO(g). Yield: 135.1 mg (0.3223 mmol, 53%). FTIR, ν_{NO} (cm^{-1}): 1638 (KBr matrix, $\Delta\nu_{NO}$: 29 cm^{-1}); 1641 (THF, $\Delta\nu_{NO}$: 29 cm^{-1}), 1648 (CH_2Cl_2, $\Delta\nu_{NO}$: 31 cm^{-1}). ^{15}N NMR (50.7 MHz, THF-d_8, δ from CH_3NO_2): 688.

[Co(LN$_4$^{PhCl}H$_2$)(NO)$_2$]BF$_4$, {Co(NO)$_2$}^{10} (3). To a 2 mL THF solution of black $[Co_2(\mu\text{-}Cl)_2(NO)_4]$ (31.7 mg, 0.103 mmol) was added a 3 mL THF solution of yellow-tinted dark brown LN$_4$^{PhCl}H$_2$ (68.0 mg, 0.205 mmol). There was no significant color change upon mixing reactants; however, light brown insolubles formed within 1 min of stirring. After 2.5 h, the solution was filtered to afford the product as a brown solid (64.0 mg, 0.132 mmol, 64%, verified by IR: ν_{NO}: 1864, 1782 cm^{-1}, KBr). To corroborate results from reactivity studies, exchange of Cl^- for BF_4^- was performed. To a 3 mL MeOH solution containing Et_4NBF_4 (22.3 mg, 0.103 mmol), was added a 4 mL MeOH solution of dark brown **3-Cl** (25.0 mg, 0.0515 mmol). After the initial addition a slight darkening in color occurred. After 30 min mixing at RT, red-brown insolubles were noted. The solution was stirred further for 1.5 h and the mixture was filtered to afford deep red-brown insoluble product (14.2 mg) and a brown colored filtrate. The filtrate volume was reduced to ~2 mL and then placed at -20 °C overnight. Filtering this cooled solution led to an additional 7.9 mg of insoluble product (total: 22.1 mg; 0.0412 mmol, 80%). FTIR (KBr matrix), ν_{max} (selected peaks, cm^{-1}): 3328 (m, ν_{NH}), 1859 (s, ν_{NO}), 1793 (vs, ν_{NO}), 1052 (vs, ν_{BF}). ^{1}H NMR (400 MHz, CD_3OD, δ from residual protio solvent): 9.28 (s, 1H), 8.07 (s, 1H), 7.54 (s, 1H), 7.27 (s, 1H), 6.62 (s, 1H). HRMS-ESI (*m/z*): $[M]^+$ calcd for $C_{16}H_{12}Cl_2CoN_6O_2$ (relative abundance), 448.973 (100.0), 450.970 (63.9), 449.976 (17.3), 451.973 (11.1), 452.967 (10.2); found, 448.973 (100.0), 450.970 (64.1), 449.976 (16.8), 451.973 (10.9), 452.967 (9.8).

Reactivity:

Reaction of 1 with HBF$_4$•Et$_2$O. To a red-tinted dark brown THF solution (1.5 mL) of **1** (15.0 mg, 0.0359 mmol) was added 6.35 μL (0.0463 mmol) of HBF$_4$•Et$_2$O in 1 mL of THF. The resulting solution remained homogeneous and dark brown but became yellow-tinted over time. The reaction mixture stirred at RT for 24 h. FTIR (KBr) was used to monitor the reaction, and a spectrum was obtained at t = 0.5, 2.5, 3.5, and 24 h (see Figures S8 and S9 for spectrum at 0.5 and 24 h, respectively; 2.5 and 3.5 h did not show any significant differences from the 0.5 h spectrum). After 24 h, the products were dried *in vacuo*, leaving a dark brown sticky residue. The products from this reaction were characterized by UV-vis and ESI-MS. An analogous smaller scale reaction (complex **1**: 6.0 mg, 0.014 mmol; HBF$_4$: 2.53 μL, 0.0186 mmol) was monitored *in situ* by ^{1}H NMR spectroscopy (298 K, 400 MHz) at t = 0.17, 1, 3, 5, 24, 48, 72, and 96 h (see Figures S10-S12 for 0.17, 1, and 24 h).

Reaction of 1-^{15}NO with HBF$_4$•Et$_2$O. The reaction with the isotopically-labeled complex **1-^{15}NO** was performed analogously to **1** except for using **1-^{15}NO** (10.0 mg, 0.0239 mmol) and 4.23 μL (0.0308 mmol) of HBF$_4$•Et$_2$O; total THF reaction volume was 2 mL. The reaction was monitored by FTIR (KBr) at t = 0.5, 2.5, 3.5, and 24 h and by NMR at t = 0.17, 1, 3, 5, 24, 48, 72, and 96 h.

UV-vis monitor of the reaction of 1 with [Fe(TPP)Cl]. A 1 mM stock solution of [Fe(TPP)Cl] was prepared in THF. After a THF blank was recorded at 298 K, a 0.025 mL aliquot of the [Fe(TPP)Cl] stock solution was added to 3.000 mL of THF in a quartz cuvette, and the UV-vis spectrum was recorded, which matched the literature value.[8] No changes occurred in the UV-vis spectrum over 30 min. To this cuvette was then added a 0.025 mL aliquot of a 1 mM THF stock solution of the $\{CoNO\}^8$ (**1**), yielding a 1:1 stoichiometric ratio of [Fe(TPP)Cl]:**1** to initiate the reaction. The UV-vis was monitored for 24 h (intervals used: 2 min cycles in the first 2 h; 30 min cycles for the next 24 h, see Figure S6 for 24 h trace – no changes after this time).

UV-vis monitor of the reaction of 1 with [Fe(TPP)Cl] in the presence of HBF_4•Et_2O. The above conditions were replicated and no reaction was noted within 24 h at T = 298 or 310 K. A 1 mM stock solution of HBF_4•Et_2O in THF was prepared, and a 0.025 mL aliquot of this solution was added to the cuvette (1:1:1 stoichiometric ratio of **1**/ [Fe(TPP)Cl]/HBF_4•Et_2O). The UV-vis spectrum was monitored for 22 h (intervals used: 1 min cycles for the first 30 min; 2 min cycles for the next 1 h; 30 min cycles for t = 1.5 h – 22 h).

Bulk reaction of 1 with [Fe(TPP)Cl]. A solution of [Fe(TPP)Cl] (33.7 mg, 0.0479 mmol) was prepared in 1 mL of THF. To this solution was added a 3 mL THF solution containing **1** (20.0 mg, 0.0478 mmol) and the reaction was stirred under dark conditions at RT for 24 h. After this time an IR was taken, which revealed ***no reaction*** as evidenced by the strong ν_{NO} band of **1**. Then, a 0.5 mL THF solution containing HBF_4•Et_2O (6.51 μL, 0.0474 mmol) was added to the reaction mixture. This solution was allowed to mix at RT for 24 h, which indicated the presence of [Fe(TPP)NO] by FTIR (KBr matrix, ν_{NO} = 1698 cm^{-1}; disappearance of the ν_{NO} of **1** at 1667 cm^{-1}) and EPR spectroscopy (see Figure S7). A similar spectrum was observed at t = 48 h. After this point, the THF was removed *in vacuo* to afford a dark brown purple residue. This residue was stirred in 3 mL of MeOH for 1 h and was then filtered to yield a deep purple solid identified to be [Fe(TPP)NO] (29.4 mg, 0.0421 mmol, 88%). The same result was obtained using **1-^{15}NO** (15.0 mg, 0.0358 mmol), [Fe(TPP)Cl] (25.2 mg, 0.0358 mmol), and HBF_4•Et_2O (4.87 μL, 0.0358 mmol) affording 22.5 mg of [Fe(TPP)^{15}NO] (0.0322 mmol, 90% yield) as confirmed by FTIR (KBr matrix, ν_{NO}: 1667 cm^{-1}, $\Delta\nu_{NO}$: 31 cm^{-1}) and EPR spectroscopy (see Figure S7).

Bulk reaction of 1 with Ph_3P. This method was adapted based on a published procedure for O-atom transfer from Fe-coordinated nitrite to Ph_3P.[5b,9] To a 2.000 mL THF:H_2O (10:1) solution of **1** (15.0 mg, 0.0359 mmol) was added a solution of Ph_3P (18.8 mg, 0.0717 mmol) in 1.500 mL THF:H_2O (10:1), and the reaction stirred at RT for 24 h under anaerobic conditions. After this time, the solution remained red-tinted dark brown with little to no insolubles noted. The reaction mixture was monitored by HPLC at t = 1 h, 3 h, 5 h, and 24 h, and a ^{31}P NMR spectrum was obtained at t = 24 h. Analysis indicated trace Ph_3P=O (small peak at retention time (t_r): 4.7 min) in the HPLC chromatogram (Figure S19). No P-containing peaks were observed in the ^{31}P NMR spectrum. At t = 24 h, a 0.500 mL THF:H_2O (10:1) solution containing HBF_4•Et_2O (6.35 μL, 0.0466 mmol) was added to the reaction mixture. After 1 h, the solution was yellow-tinted deep brown in color and by 24 h, the solution had lightened in color to a yellow-tinted transparent brown homogeneous solution. The reaction mixture was monitored by HPLC at t = 1 h, 3 h, 5 h, and 24 h after addition. At 24 h, the solvent was removed in vacuo, leaving a yellow-tinted brown residue. This residue was treated with Et_2O for 30 min (4 × 5 mL) and then filtered, yielding a yellow filtrate (17.2 mg after Et_2O removal) and a brown sticky solid (17.8 mg). A ^{31}P

NMR spectrum was obtained for both the Et_2O soluble (unreacted Ph_3P) and Et_2O insoluble (unreacted Ph_3P, Ph_3P=NH, Ph_3P=O) fractions. Based on HPLC, a 20% yield of Ph_3P=O (LRMS-ESI, $\{Ph_3P{=}O + H^+\}^+$, *m/z* 279.1; calcd: 279.1) was noted. Utilizing 10 equiv of PPh_3 afforded a 27% yield of PPh_3O.

The modest yield of Ph_3P=O may be due to coordination to Co. To quantify total Ph_3P=O, the reaction was performed in the same manner with the same quantities as stated above with the exception of adding excess HBF_4•Et_2O to remove any potential bound phosphine oxide. After 24 h mixing, a 500 μL THF:H_2O (10:1) solution containing HBF_4•Et_2O (122.0 μL, 0.8969 mmol, 25 equiv with respect to **1**) was added to the $\{CoNO\}^8$/2 Ph_3P/H^+ reaction mixture. This led to an immediate color change to deep yellow with no noted insolubles. No further changes occurred after stirring at RT for 2 h. This mixture was then analyzed by HPLC, which revealed a 33% yield of Ph_3P=O. Identical conditions were used for the acid digest of $\{CoNO\}^8$/10 PPh_3/H^+ except for using a 500 μL THF:H_2O (10:1) solution of HBF_4•Et_2O (488.5 μL, 3.590 mmol, 100 equiv with respect to **1**); yield = 37%.

Bulk Reaction of 1 with O_2(g). A solution of **1** (15.0 mg, 0.0359 mmol) was prepared in 3 mL of MeCN:THF (1:1) and then purged with a stream of O_2(g) for 1.5 min at RT. Addition of O_2(g) resulted in an immediate albeit slight color change; the solution became darker brown (red-tinted) and no insolubles were noted. The reaction was stirred at RT under O_2(g) atmosphere and aliquots of the reaction mixture were taken at 24 h and 72 h. The FTIR spectrum of each aliquot indicated disappearance of the ν_{NO} of **1** after 24 h. The reaction mixture was dried *in vacuo*, yielding a red-brown solid (total recovered: 15.4 mg) that was a mixture of $[Co(LN_4^{PhCl})(MeCN)(\eta^1\text{-}ONO_2)]$ (**2**) and $[Co(LN_4^{PhCl})(MeCN)(NO_2)]$. Formation of **2** and the Co-NO_2 complex upon oxidation of $\{CoNO\}^8$ complex **1** is not an unprecedented phenomenon.[10] Product **2** was obtained in 63% yield based on NMR integration. IR stretching frequencies have been assigned based on known ranges reported for typical Co-η^1-ONO_2 and Co-NO_2 complexes.[11] FTIR of peaks assigned to complex **2** (KBr matrix), ν_{max} (cm^{-1}): 2302 (w, $\nu_{C\equiv N}$), 1509 (m, ν_{NO}), 1489 (m, ν_{NO}), 1270 (s, ν_{NO}), 1046 (s, ν_{NO}). ^{1}H NMR of peaks assigned to **2** (400 MHz, CD_3CN, δ from residual protio solvent: 8.26 (s, 1H), 8.01 (s, 1H), 7.77 (s, 1H), 7.17 (d, 1H), 6.51 (d, 1H).

Structural Data

X-ray Crystallographic Data Collection and Structure Solution and Refinement. Dark brown crystals of $[Co(LN_4^{PhCl})(NO)]$ (**1**) were grown under anaerobic conditions by slow diffusion of Et_2O into a 2-MeTHF solution of **1** at -20 °C. Red crystals of $[Co(LN_4^{PhCl})(\eta^1\text{-}ONO_2)]$ (**2**) were grown under pseudo-anaerobic conditions by slow diffusion of Et_2O into a THF:MeCN (1:1) solution of **1** at 8 °C, resulting in single crystals of nitrato complex **2** due to oxidation of the NO ligand in **1**. Suitable crystals were mounted on a glass fiber. The X-ray intensity data were measured at 100 K on a Bruker SMART APEX II X-ray diffractometer system with graphite-monochromated Mo Kα radiation (λ = 0.71073 Å) using ω-scan technique controlled by the SMART software package.[12] The data were collected in 1464 frames with 10 second exposure times. The data were corrected for Lorentz and polarization effects[13] and integrated with the manufacturer's SAINT software. Absorption corrections were applied with the program SADABS.[14] Subsequent solution and refinement was performed using the SHELXTL 6.1 solution package operating on a Pentium computer.[15] The structure was solved by

direct methods using the SHELXTL 6.1 software package.[16] Non-hydrogen atomic scattering factors were taken from the literature tabulations.[17] Selected data and metric parameters for complexes **1** and **2** are summarized in Table S1. Selected bond distances and angles for **1** and **2** are given in Table S2. Perspective views of the complexes were obtained using ORTEP.[18] The asymmetric unit of **1** contains one half of a discrete THF molecule, which was disordered residing on the symmetry of an inversion center with half occupancies of each atom. The B alert in the cif-check for **1** is a false alert. The B alerts in the cif-check for **2** are due to the quality of data collected (R_{int} = 0.208).

Table S1. Summary of crystal data and intensity collection and structure refinement parameters for [Co(LN_4^{PhCl})(NO)]•0.5THF (**1**•0.5THF) and [Co(LN_4^{PhCl})(MeCN)(η^1-ONO_2)] (**2**).

Parameters	**1**•0.5 THF	**2**
Formula	$C_{18}H_{14}Cl_2CoN_5O_{1.5}$	$C_{18}H_{13}Cl_2CoN_6O_3$
Formula weight	454.17	491.17
Crystal system	Triclinic	Orthorhombic
Space group	*P*-1	$P2_12_12_1$
Crystal color, habit	Dark brown	Red
a, Å	7.8436(9)	11.086(8)
b, Å	9.7124(11) Å	12.066(8)
c, Å	12.4551(13)	14.350(10)
α, deg	85.689(2)	90
β, deg	77.5370(10)	90
γ, deg	83.590(2)	90
V, Å^3	919.40(18)	1919(2)
Z	1	4
$\rho_{calcd,}$ g/cm^3	1.641	1.700
T, K	100(2)	100(2)
abs coeff, μ (Mo Kα), mm^{-1}	1.246	1.208
θ limits, deg	2.11-27.00	2.21-25.05
total no. of data	11541	18909
no. of unique data	3999	3405
no. of parameters	271	272
GOF of F^2	1.052	1.016
R_1,[a] %	4.94	7.53
wR_2,[b] %	13.18	11.95
max, min peaks, e/Å^3	1.108, -0.683	0.375, -0.465

[a]$R_1 = \Sigma| |F_O| - |F_c| | / \Sigma |F_O|$; [b]$wR_2 = \{\Sigma[w(F_o^2 - F_c^2)^2]/\Sigma[w(F_o^2)^2]\}^{1/2}$

Table S2. Selected bond distances (Å) and bond angles (deg) for [Co(LN_4^{PhCl})(NO)]•0.5THF (**1**•0.5THF) and [Co(LN_4^{PhCl})(MeCN)(η^1-ONO_2)] (**2**).

1•0.5THF		**2**	
Co1-N1	1.927(3)	Co1-N1	1.936(7)
Co1-N2	1.897(3)	Co1-N2	1.901(7)
Co1-N3	1.892(3)	Co1-N3	1.884(7)
Co1-N4	1.911(3)	Co1-N4	1.915(7)
Co1-N5	1.798(3)	Co1-N5	1.907(8)
N5-O1	1.172(4)	Co1-O1	1.904(6)
		N6-O1	1.227(9)
		N6-O2	1.237(10)
		N6-O3	1.239(9)
O1-N5-Co1	124.4(3)	N1-Co1-N2	83.0(3)
N1-Co1-N2	83.06(12)	N1-Co1-N3	166.5(3)
N1-Co1-N3	162.15(13)	N1-Co1-N4	109.5(3)
N1-Co1-N4	106.63(13)	N1-Co1-N5	90.1(3)
N1-Co1-N5	96.97(13)	N1-Co1-O1	93.0(3)
N2-Co1-N3	82.74(12)	N2-Co1-N3	83.6(3)
N2-Co1-N4	157.59(13)	N2-Co1-N4	167.3(3)
N2-Co1-N5	101.93(13)	N2-Co1-N5	90.9(3)
N3-Co1-N4	83.25(13)	N2-Co1-O1	86.9(3)
N3-Co1-N5	96.50(13)	N3-Co1-N4	84.0(3)
N4-Co1-N5	96.97(13)	N3-Co1-N5	91.4(3)
		N4-Co1-N5	87.0(3)
		O1-Co1-N3	85.0(3)
		O1-Co1-N4	94.4(3)
		O1-Co1-N5	175.9(3)
		O1-N6-O2	124.3(8)
		O1-N6-O3	118.6(9)
		O2-N6-O3	117.0(10)

X-Ray Absorption Spectroscopy (XAS): Solid $\{CoNO\}^8$ **1** was prepared anaerobically at a 3:1 stoichiometric dilution with boron nitride, loaded into transmission cells wrapped with kapton tape and immediately frozen in liquid nitrogen. Two independent duplicates were prepared to ensure spectral reproducibility. XAS data were collected at the Stanford Synchrotron Radiation Light Source (SSRL), on beamline 7-3, and the National Synchrotron Light Source (NSLS), on beamline X3-A. Beamline 7-3 was equipped with a Si[220] double crystal monochromator and beamline X3-A was equipped with a Si[111] monochromator; both beamlines were equipped with harmonic rejection mirrors. During data collection, the sample at SSRL was maintained at 10 K using an Oxford Instruments continuous-flow liquid helium cryostat and the sample at NSLS was maintained at 24 K using a helium Displex cryostat. Transmission spectra, collected with a simultaneous Co foil spectrum for monochromator calibration, were measured at both locations using nitrogen gas ionization chamber detectors placed in series. The first inflection point of the Co foil spectrum was assigned to 7709.5 eV. At both facilities, XAS spectra were collected in 5 eV increments in the pre-edge region (7542-7702 eV), 0.25 eV increments in the edge region (7702-7780 eV) and 0.05 $Å^{-1}$ increments in the extended X-ray absorption fine structure (EXAFS) region. Data were collected to k = 14.0 $Å^{-1}$ and integrated from 1 to 25 seconds in a k^3-weighted manner for a total scan length of approximately 40 minutes. Spectra displayed in Figure 2 of the main paper represent the average of two independent spectra.

XAS data were processed using the Macintosh OS X version of the EXAFSPAK program suite integrated with Feff v7.2 for theoretical model generation.[19] Data reduction utilized a polynomial function in the pre-edge region and a four point cubic spline throughout the EXAFS region for background signal removal. Data were converted to k space using a Cobalt E_0 value of 7725 eV. Normalized XANES data were subjected to pre-edge analysis. Edge inflection energies were calculated as the maximum of the first derivative of the XANES spectra. Only spectra collected using the higher resolution Si[220] monochromator crystals were subjected to edge analysis. Pre- and post-edge splines were fit to the experimental spectra within the energy ranges of 7707-7718 eV. The extrapolated line was then subtracted from raw data to yield baseline corrected spectra. Pre-edge features were modeled using pseudo-Voigt line shapes (simple sums of Lorentzian & Gaussian functions) and the energy position measured at the peak height; the full width at half-maximum (fwhm) and the peak heights for each transition were varied. A fixed 50:50 ratio of Lorentzian to Gaussian function successfully reproduced the spectral features of the pre-edge transitions.[20] Peak transition areas were determined for all spectra over the energy range of 7707-7718 eV using the program Kaleidagraph.[21] Normalized areas are represented in units of 10^{-2} eV.[22]

EXAFS data were fit using single scattering theoretical model amplitudes and phase functions. The k^3- weighted EXAFS was truncated between 1.0 and 13 $Å^{-1}$ for filtering purposes and Fourier transformed for display. This k range corresponds to a spectral resolution of 0.13 Å for all Co-ligand interactions; therefore, only independent scattering environments at distances > 0.13 Å were considered resolvable in the EXAFS fitting analysis. A scale factor (Sc) of 0.98 and a threshold shift (ΔE_0) value of -11.3, calibrated by fitting crystallographically characterized cobalt complexes, were used in simulating the complex **1** sample. During the simulations, only the bond length and Debye-Waller disorder factor were allowed to vary, Sc and E_0 were held constant and the coordination number for the fit manually varied in 0.5 value increments. Criteria for judging the best-fit simulation utilized both the lowest mean-square deviation between data and fit (F′), corrected for the number of degrees of freedom, and a reasonable Debye-Waller

factor (σ^2 < 0.006 Å^2).[23] The final fitting results listed in Table S3 are from averaged values obtained from simulations of raw unfiltered data.

Table S3. Summary of best-fit simulations to Co EXAFS.[a]

Data	Nearest Neighbor Ligand Environment[b]				Long Range Ligand Environment[b]								
	Atom[c]	R(Å)[d]	CN[e]	σ^2[f]	Atom[c]	R(Å)[d]	CN[e]	σ^2[f]	Atom[c]	R(Å)[d]	CN[e]	σ^2[f]	*F*[g]
Complex **1**	N	1.88	4.5	4.64	C	2.76	4.5	1.90	C	3.92	4.5	3.16	1.12

[a] Data were fit over a *k* range of 1 to 13.0 Å^{-1}.
[b] Independent metal-ligand scattering environment.
[c] Scattering atoms: N (nitrogen) C (carbon).
[d] Average metal-ligand bond length from two transmission scans.
[e] Average metal-ligand coordination number from two transmission scans.
[f] Average Debye-Waller factor in Å^2 x 10^3 from two transmission scans.
[g] Number of degrees of freedom weighted mean square deviation between data and fit.

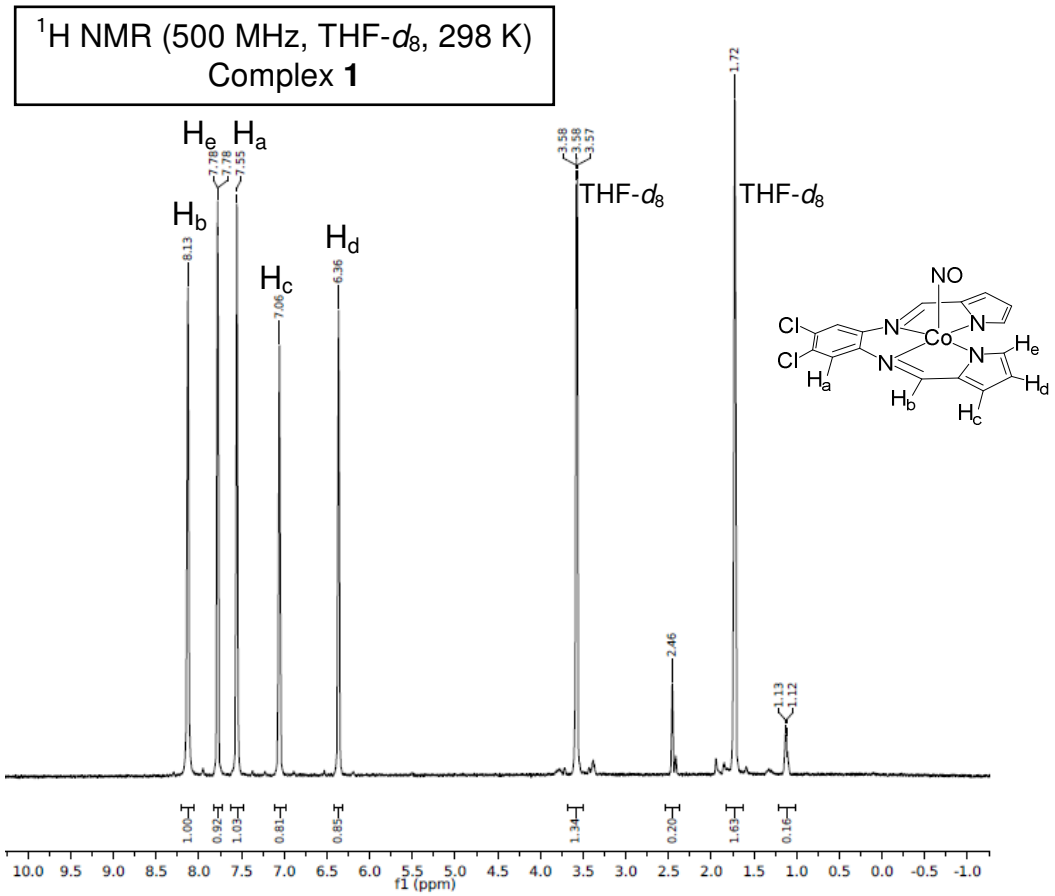

Figure S1. ^{1}H NMR spectrum of [Co(LN$_4^{PhCl}$)(NO)] (**1**) in THF-d_8 at 298 K. The peaks at 3.58 and 1.72 ppm are from residual protio solvent. The peak at 2.46 ppm is from trace H_2O.

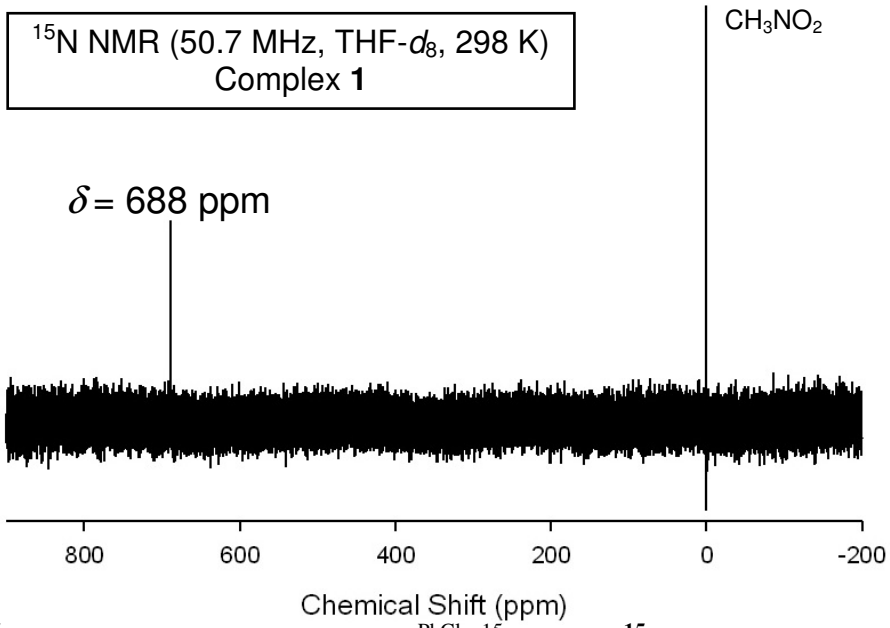

Figure S2. ^{15}N NMR spectrum of [Co(LN$_4^{PhCl}$)(^{15}NO)] (**1-^{15}NO**) in THF-d_8 at 298 K (vs. CH_3NO_2).

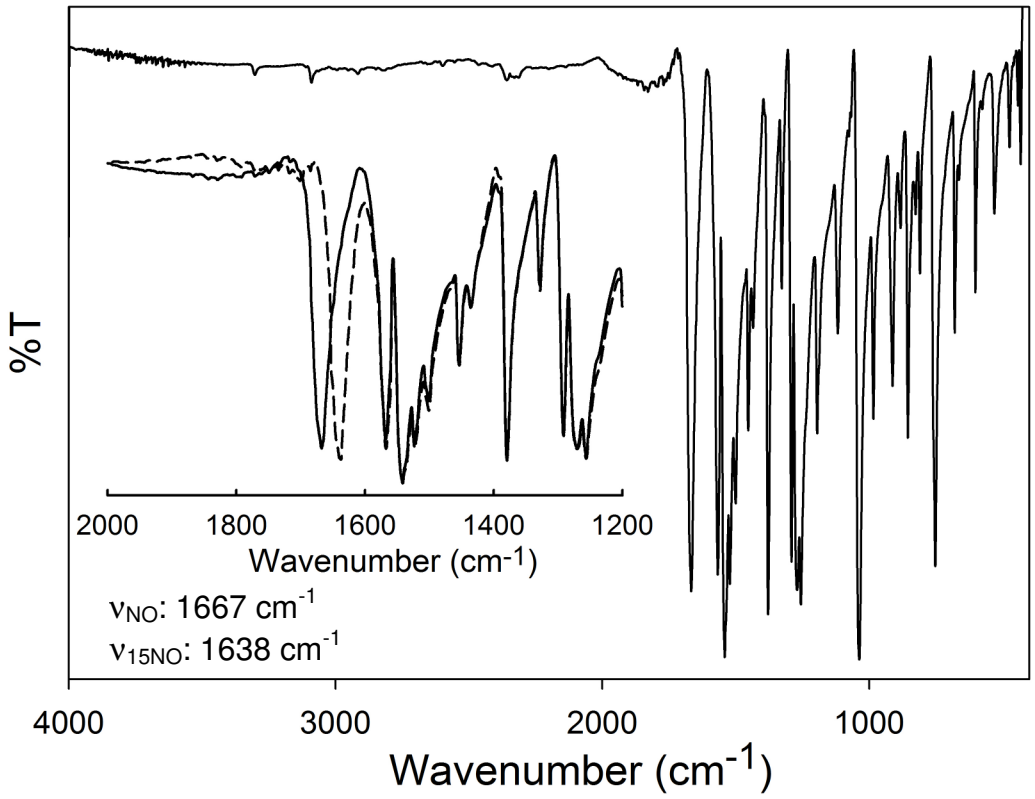

Figure S3. FTIR spectra of [Co(LN_4^{PhCl})(NO)] (**1**) (solid line) and [Co(LN_4^{PhCl})(^{15}NO)] (**1-^{15}NO**) (dashed line; inset) in a KBr matrix.

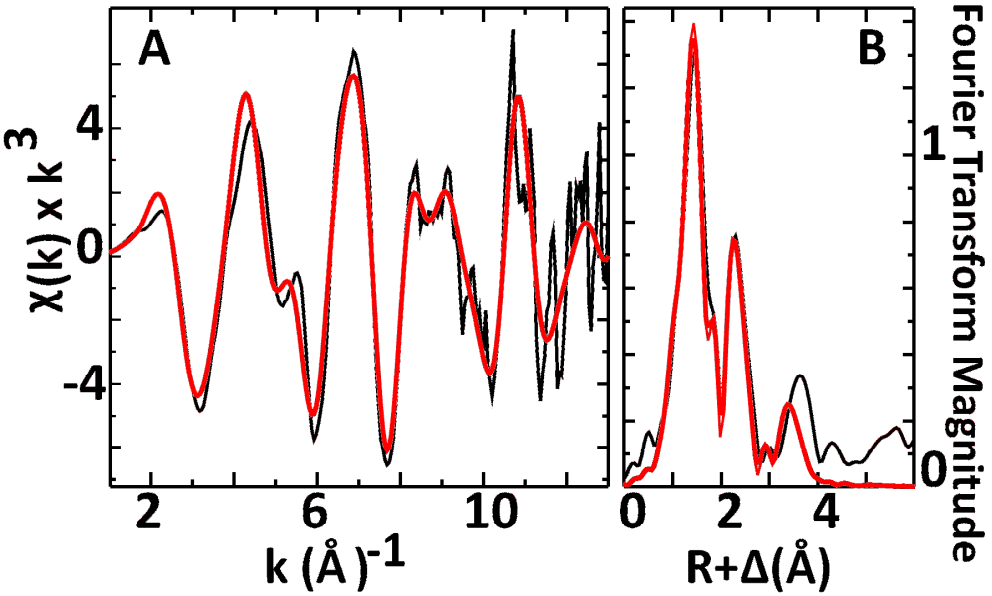

Figure S4. EXAFS and Fourier transforms of EXAFS data for {CoNO}^{8} **1**. (A): Raw EXAFS data displayed in black and best fits in red. (B): Corresponding Fourier transform plot of raw EXAFS data.

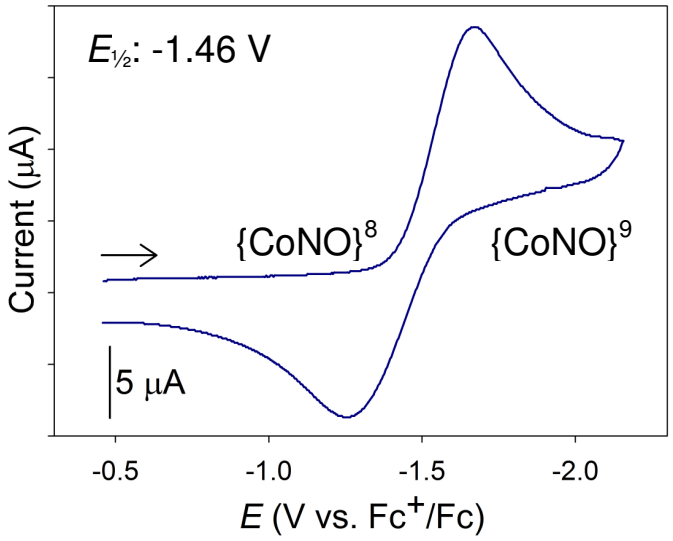

Figure S5. Cyclic voltammogram of **1** (3 mM) in THF with 0.1 M ^{n}BuN$_4$PF$_6$ as supporting electrolyte. GC working electrode; scan rate: 100 mV•s^{-1}. Arrow shows direction of scan.

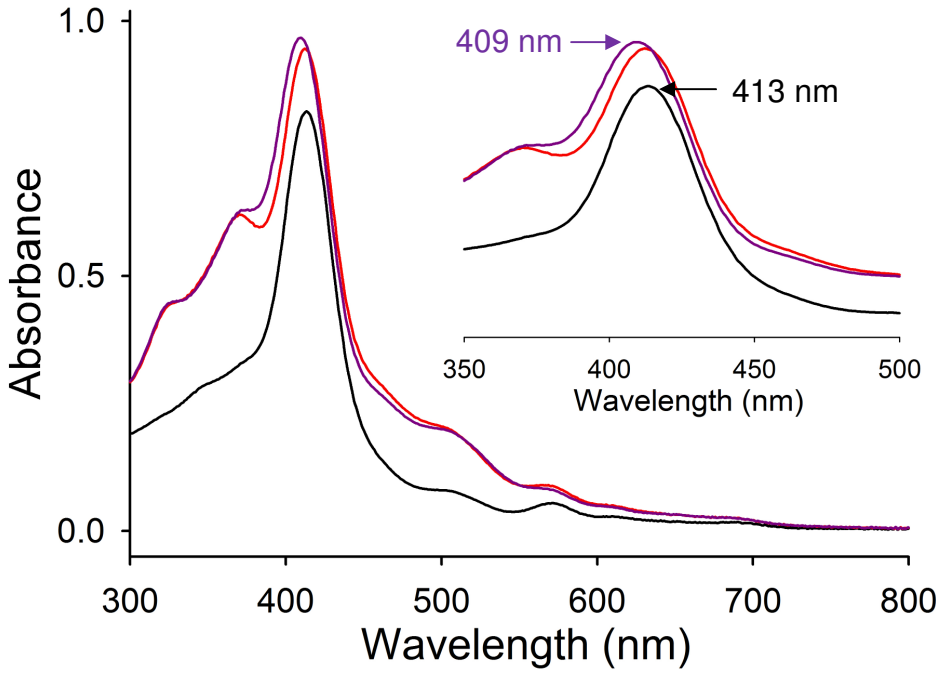

Figure S6. UV-vis spectrum of 8.2 μM [Fe(TPP)Cl] (black), [Fe(TPP)Cl] + complex **1** (1:1) after 24 h mixing (red), and [Fe(TPP)Cl] + complex **1** + HBF$_4$•Et$_2$O (1:1:1) after 4 min mixing (violet). No significant changes after this time. Reaction performed in THF at 298 K. *Inset*: expansion of the Soret band of the reaction mixture (same coloring as in full spectrum). λ_{max} for black and red traces: 413 nm; λ_{max} for violet trace: 409 nm.

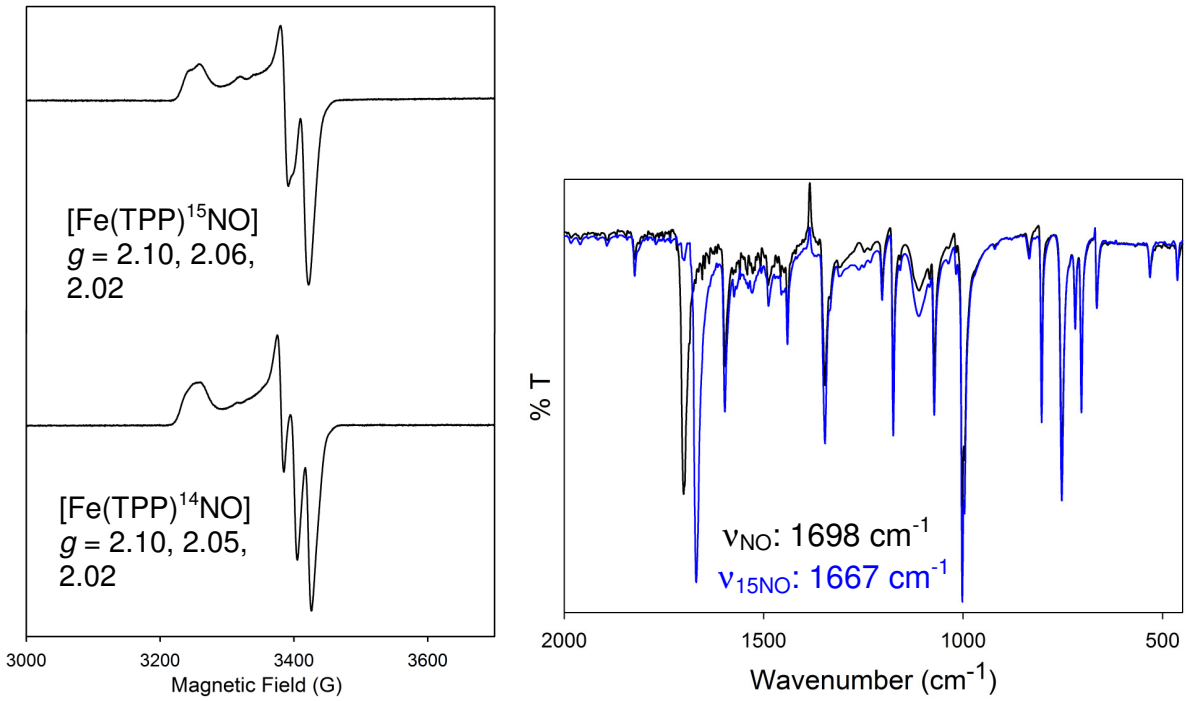

Figure S7. *Left*: X-band EPR spectrum of the reaction of **1** (bottom) or **1-^{15}NO** (top) with [Fe(TPP)Cl] showing formation of the corresponding $\{FeNO\}^7$ complex [Fe(TPP)(NO)]. *Right*: Solid-state (KBr) FTIR spectrum of the ν_{NO} region of the same reaction mixture using **1** (black) or **1-^{15}NO** (blue).

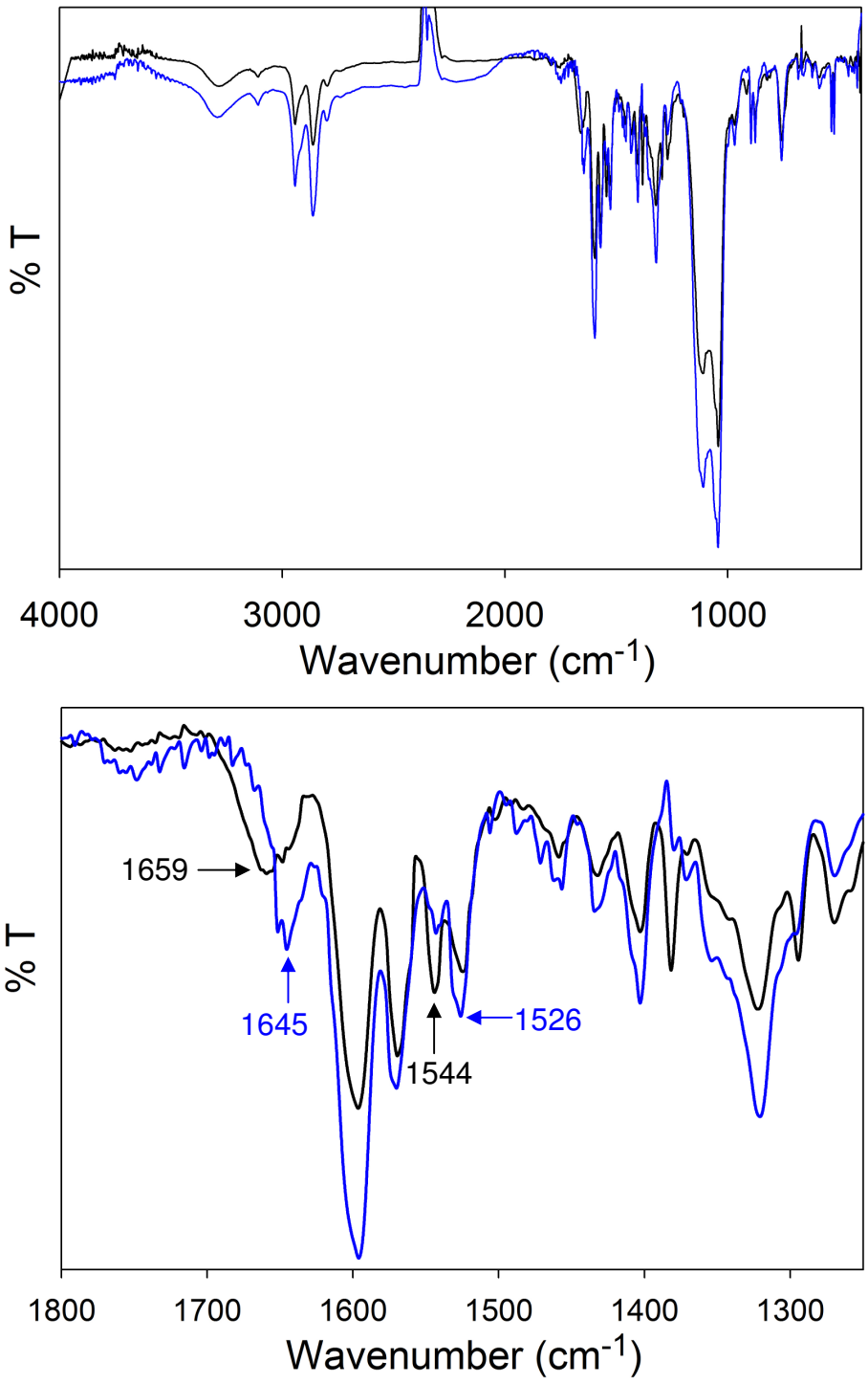

Figure S8. Solid-state FTIR spectrum of **1** + HBF_4•Et_2O (1:1.3) (black trace) and **1-^{15}NO** + HBF_4•Et_2O (1:1.3) (blue trace) after 0.5 h. *Top*: Full spectrum. *Bottom*: Expansion of ν_{NO} region. Sample measured as a KBr pellet at RT. Isotope-sensitive ν_{NO} peaks are labeled in cm^{-1}.

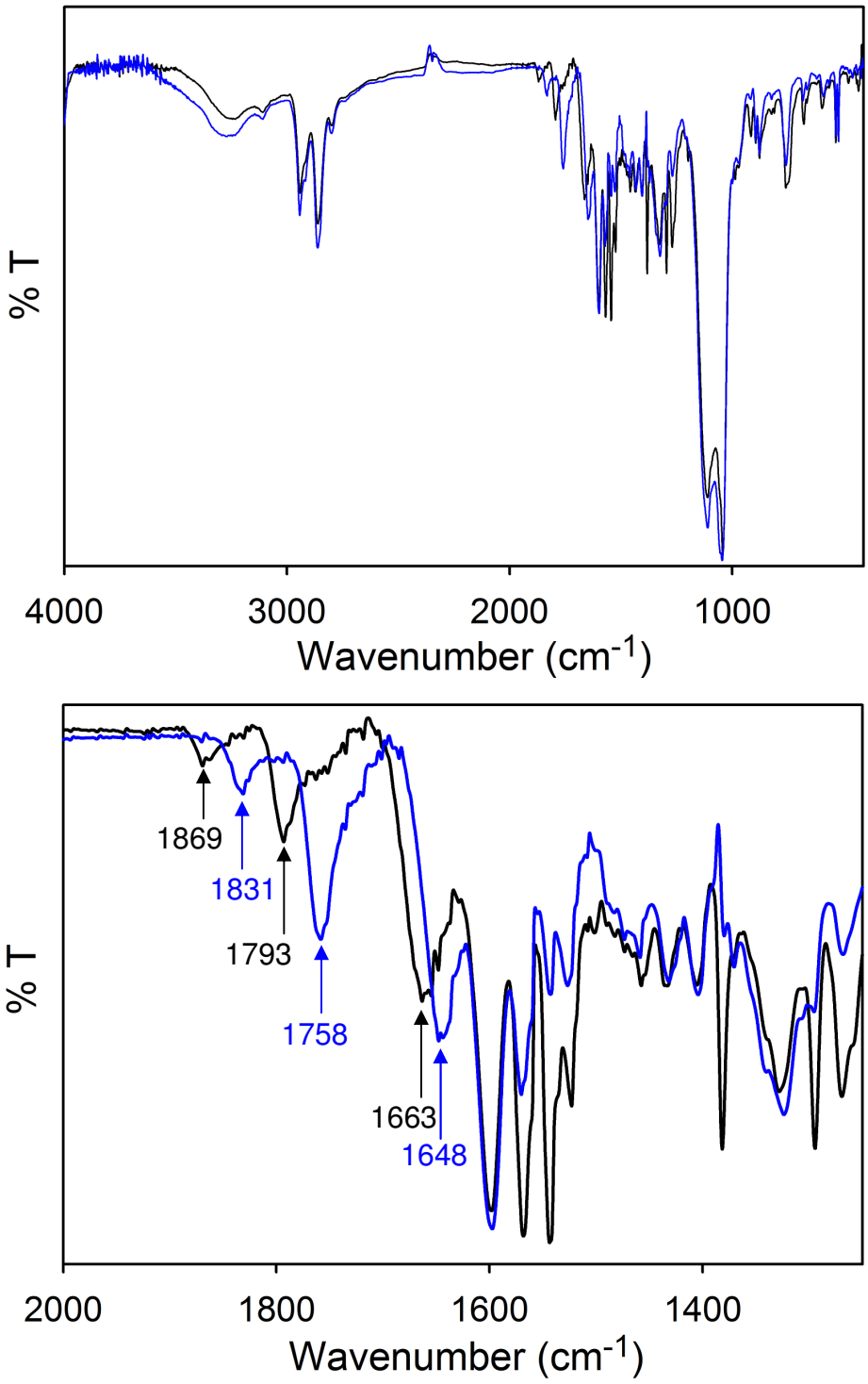

Figure S9. Solid-state FTIR spectrum of **1** + HBF_4•Et_2O (1:1.3) (black trace) and **1-^{15}NO** + HBF_4•Et_2O (1:1.3) (blue trace) after 24 h. *Top*: Full spectrum. *Bottom*: Expansion of ν_{NO} region. Sample measured as a KBr pellet at RT. Isotope-sensitive ν_{NO} peaks are labeled in cm^{-1}.

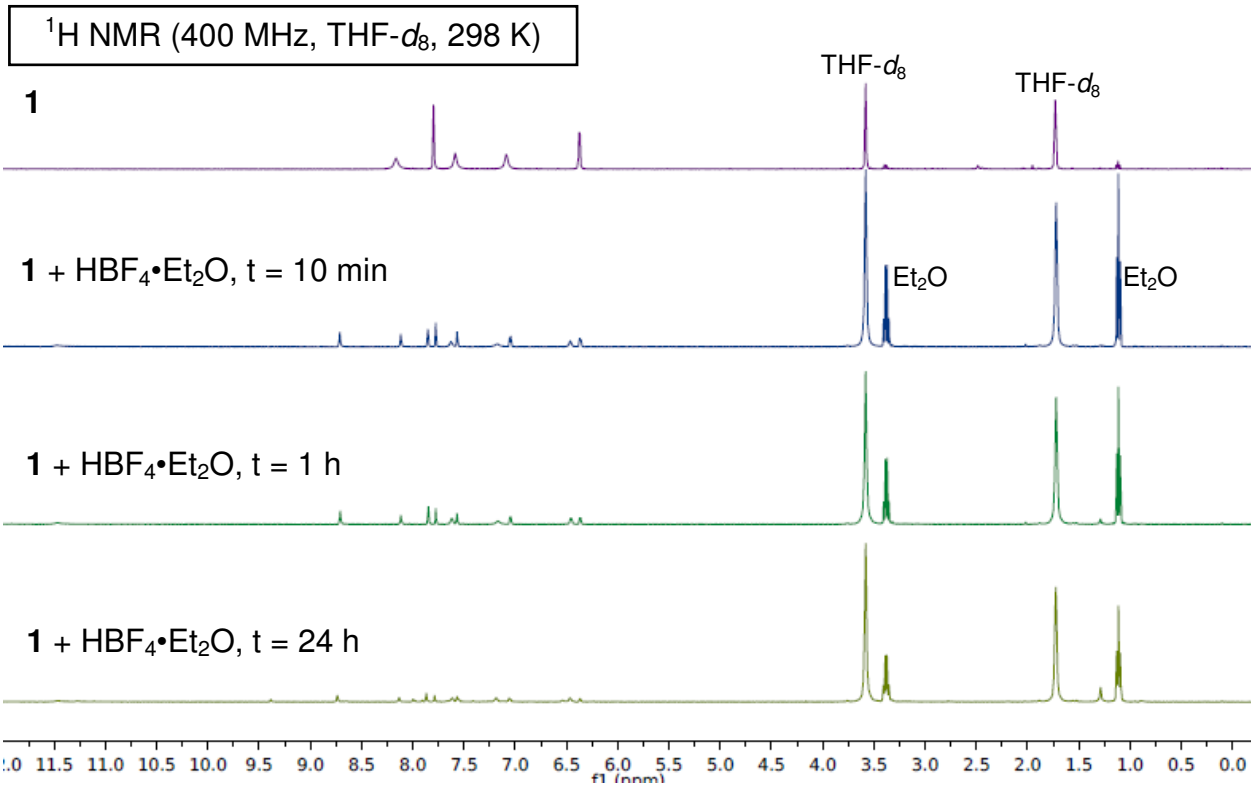

Figure S10. ^{1}H NMR spectral monitoring of the reaction of **1** and HBF_4•Et_2O (1:1.3) in THF-d_8 at 298 K. Peaks at 3.58 and 1.72 ppm are from residual protio solvent. Peaks at 3.38 (q) and 1.12 (t) ppm are from the associated Et_2O of HBF_4•Et_2O. See Figure S11 for expansion.

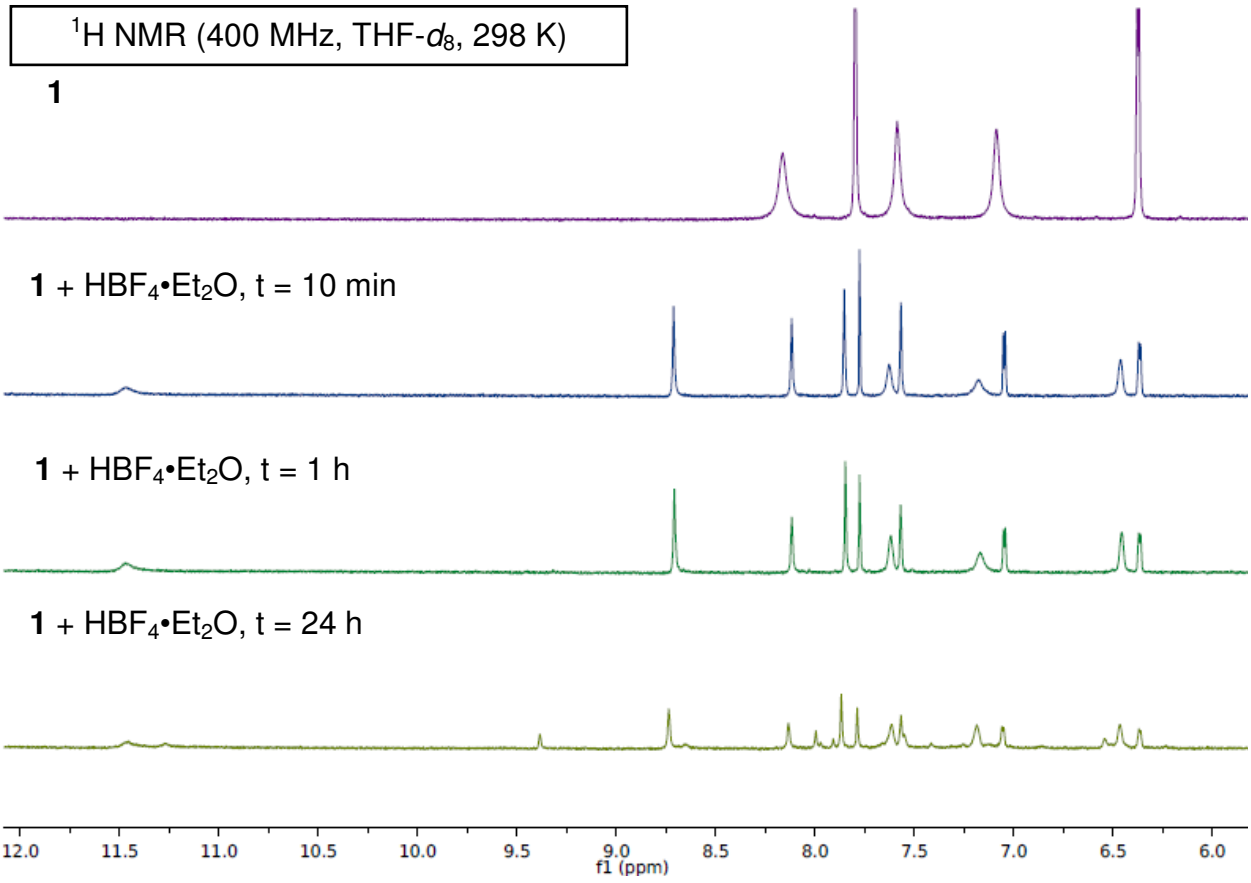

Figure S11. Expansion of the aromatic region of the ^{1}H NMR spectra from Figure S10.

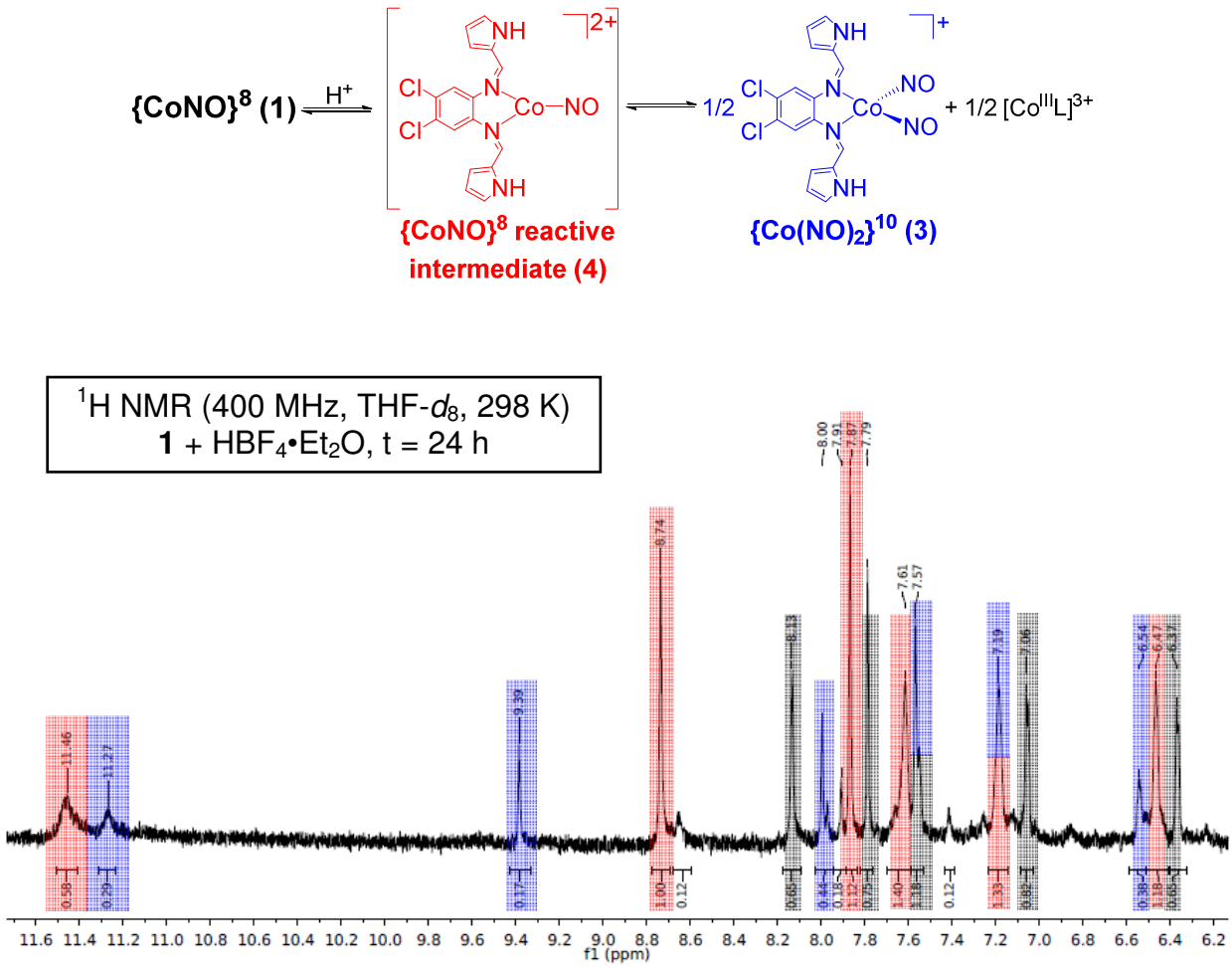

Figure S12. *Top*: color-coded reaction scheme of **1** + H^+. *Bottom*: Zoom-in of 24 h spectrum from Figure S11. Peaks are color-coded accordingly: $\{CoNO\}^8$ (**1**): gray, $\{Co(NO)_2\}^{10}$ (**3**): blue, three-coordinate $[Co(LN_4^{PhCl}H_2)(NO)](BF_4)_2$ (**4**): red, based on comparison to authentic standards except for **4**.

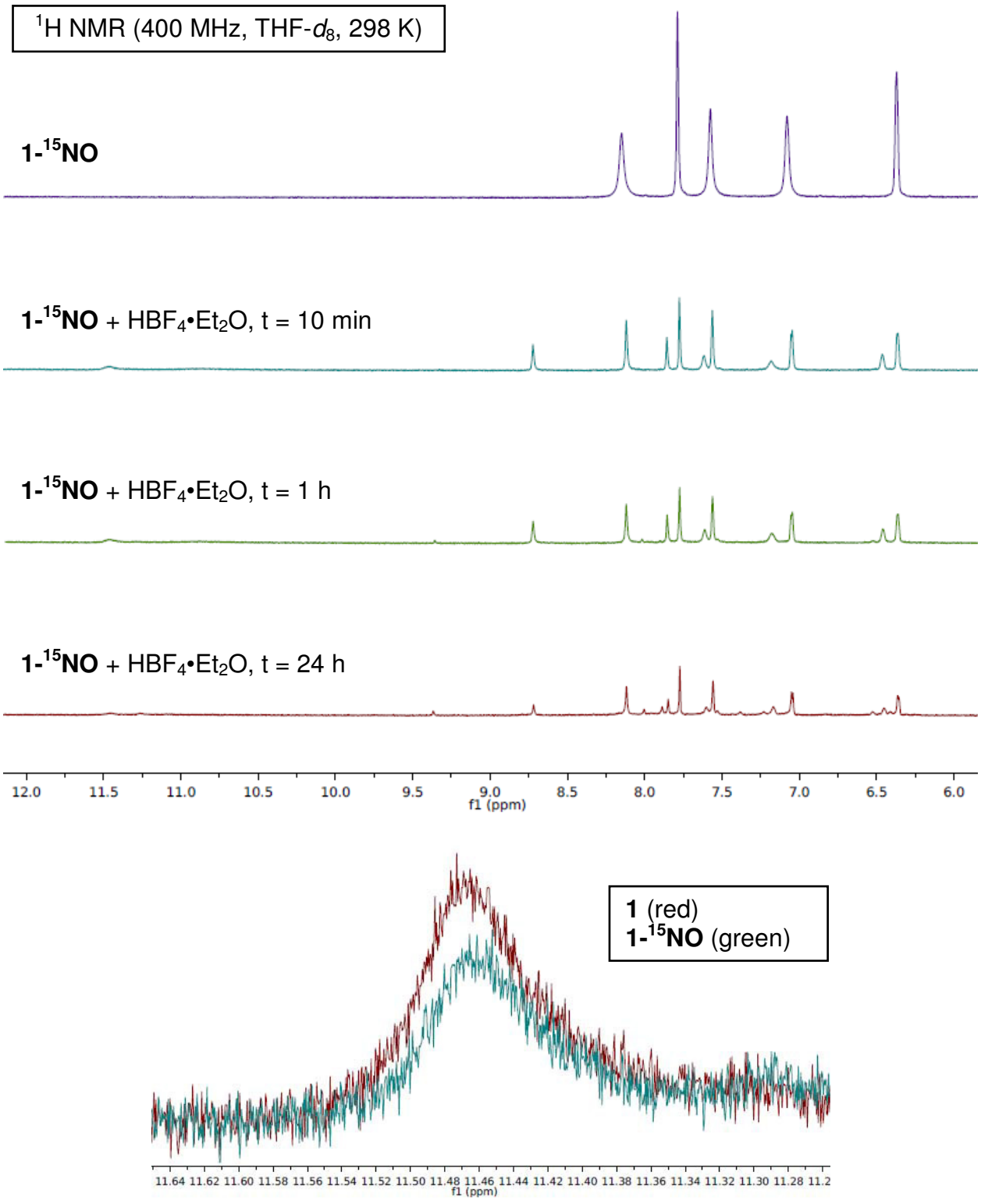

Figure S13. Aromatic region of the ^{1}H NMR monitor of the reaction of **1-^{15}NO** and HBF_4•Et_2O (1:1.3) in THF-d_8 at 298 K. Bottom figure is a zoom-in of the 11.46 ppm peak after 1 h.

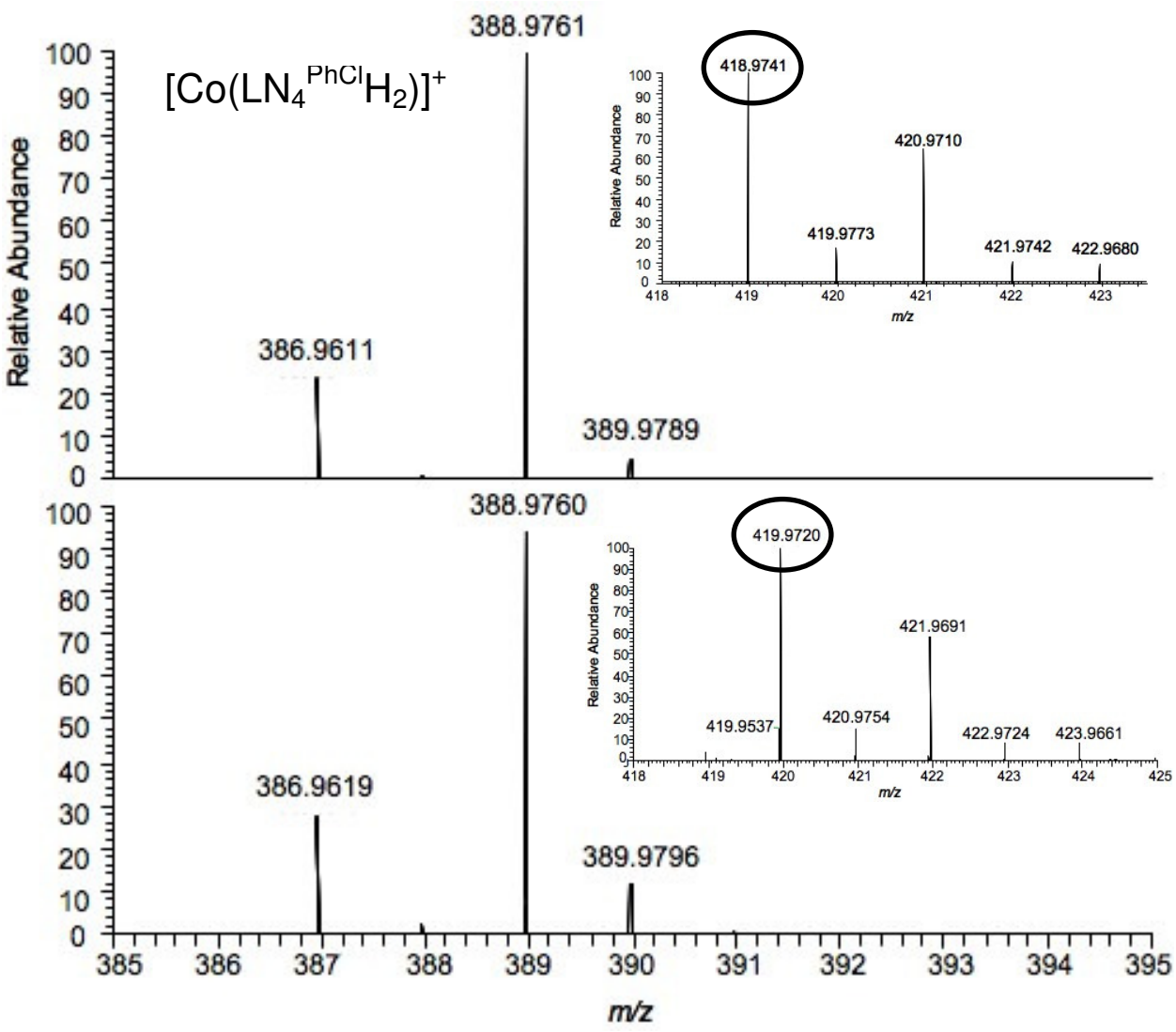

Figure S14. *Top*: High-resolution ESI-MS-MS (positive mode) of peak at *m/z*: 418.9741 (see inset) from the reaction of **1** + HBF_4•Et_2O (1:1.3). *Bottom*: ESI-MS-MS (positive mode) of peak at *m/z*: 419.9720 (see inset) from the reaction of **1-^{15}NO** + HBF_4•Et_2O (1:1.3). Samples were run in THF with an isolation width of 1 amu. The peak at *m/z*: 388.976 in both MS-MS experiments corresponds to the complex $[Co(LN_4{}^{PhCl}H_2)]^+$ via loss of NO or ^{15}NO.

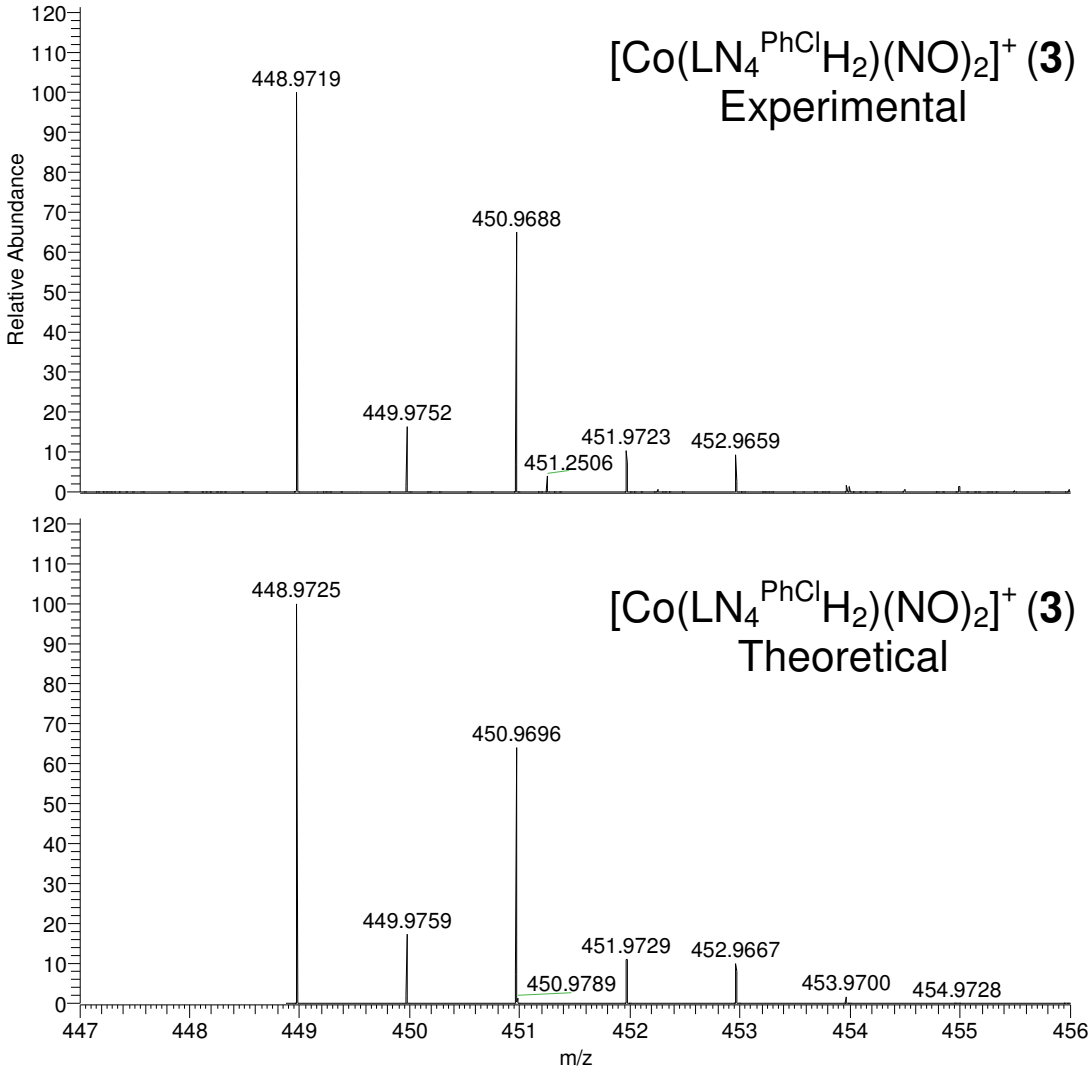

Figure S15. *Top*: High-resolution ESI-MS (positive mode) of $[Co(LN_4^{PhCl}H_2)(NO)_2]BF_4$ (**3**) from the reaction of **1** + HBF_4•Et_2O (1:1.3) after 24 h. *Bottom*: Theoretical MS for complex **3**.

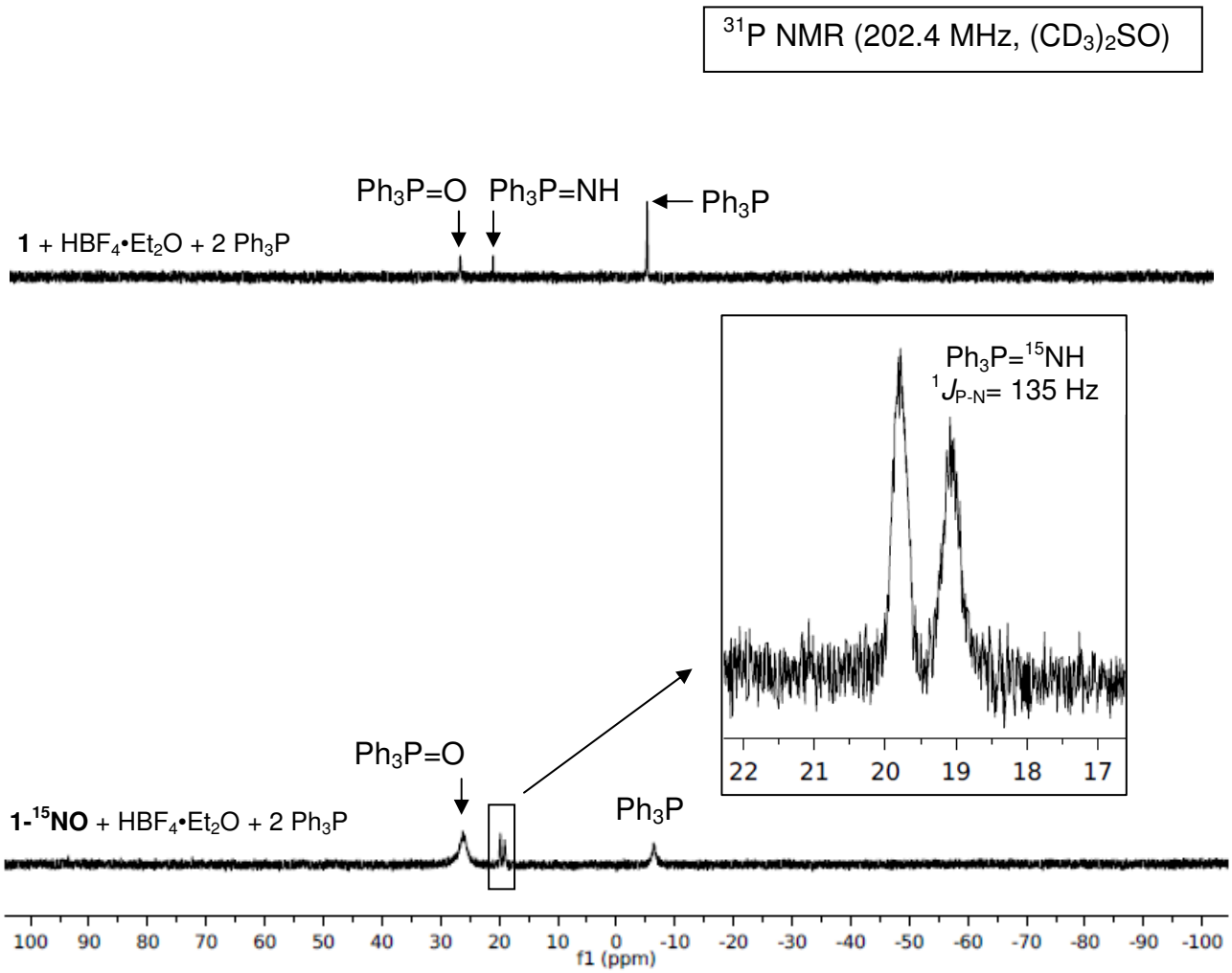

Figure S16. ^{31}P NMR spectra of the reaction of **1** + 1.3 HBF_4•Et_2O + 2 Ph_3P (top), and **1-^{15}NO** + 1.3 HBF_4•Et_2O + 2Ph_3P (bottom) after 24 h reacting at RT. All spectra recorded in $(CD_3)_2SO$ at 298 K, δ vs. external 85% H_3PO_4. *Inset for **1-^{15}NO** reaction*: expansion of the Ph_3P=^{15}NH peak showing the splitting due to the ^{15}N nucleus.

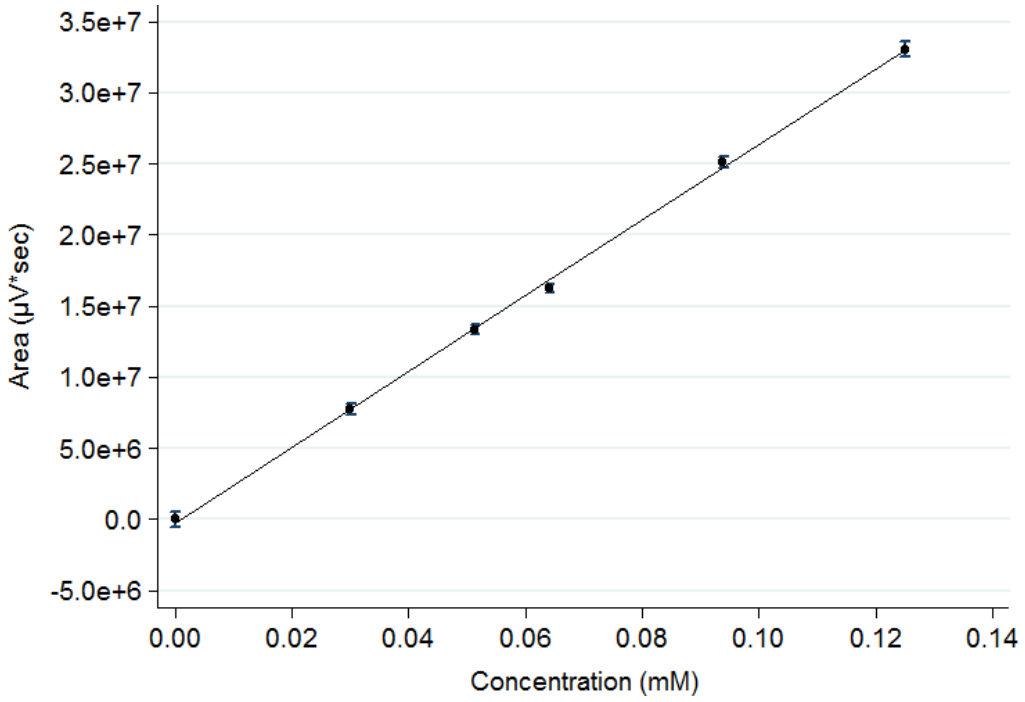

Figure S17. HPLC-generated calibration curve for $Ph_3P{=}O$ in MeCN/H_2O (65/35). Each point represents the average of three trials.

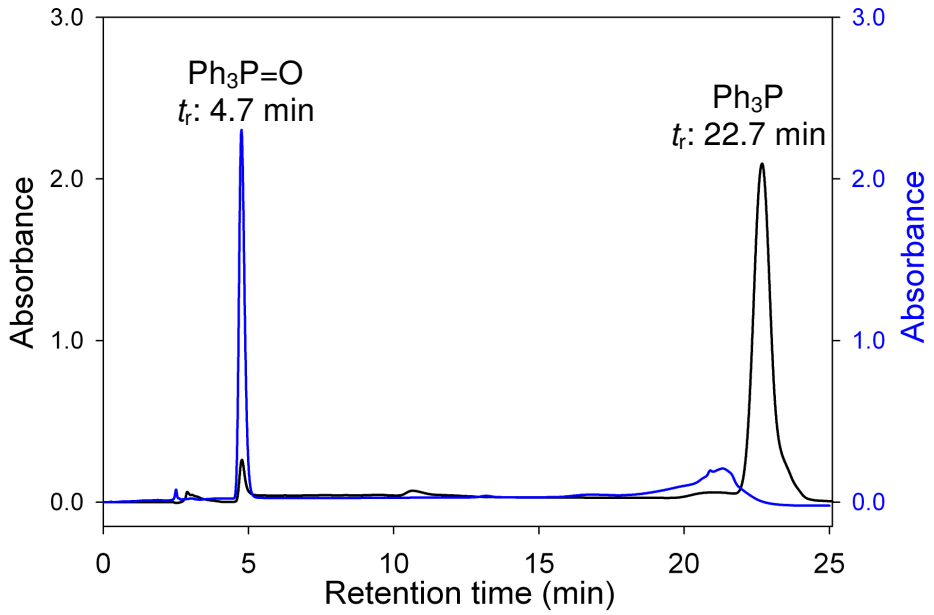

Figure S18. HPLC chromatograms of Ph_3P (t_r: 22.7 min) and $Ph_3P{=}O$ (t_r: 4.7 min) controls in MeCN/H_2O (65/35).

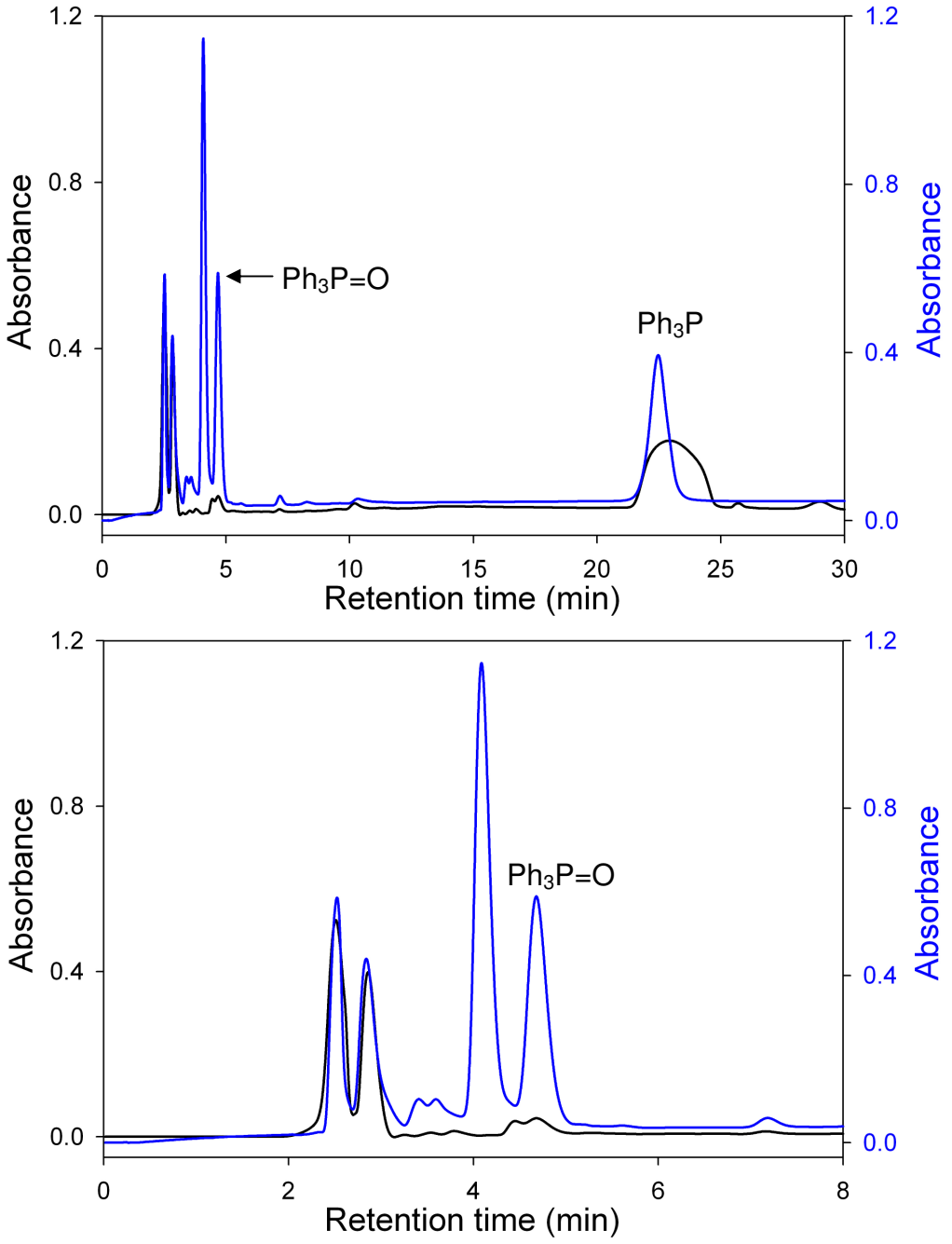

Figure S19. HPLC chromatograms of the reaction of **1** + 2 Ph_3P (*black*) and **1** + 2 Ph_3P+ 1.3 HBF_4•Et_2O (blue) after 24 h mixing at RT in THF/H_2O (10/1). *Top*: full chromatogram. *Bottom*: zoom-in of area where Ph_3P=O elutes. Peaks at 2.5, 2.9, and 4.1 min are from **1**, $LN_4^{PhCl}H_2$, and an unidentified compound, respectively.

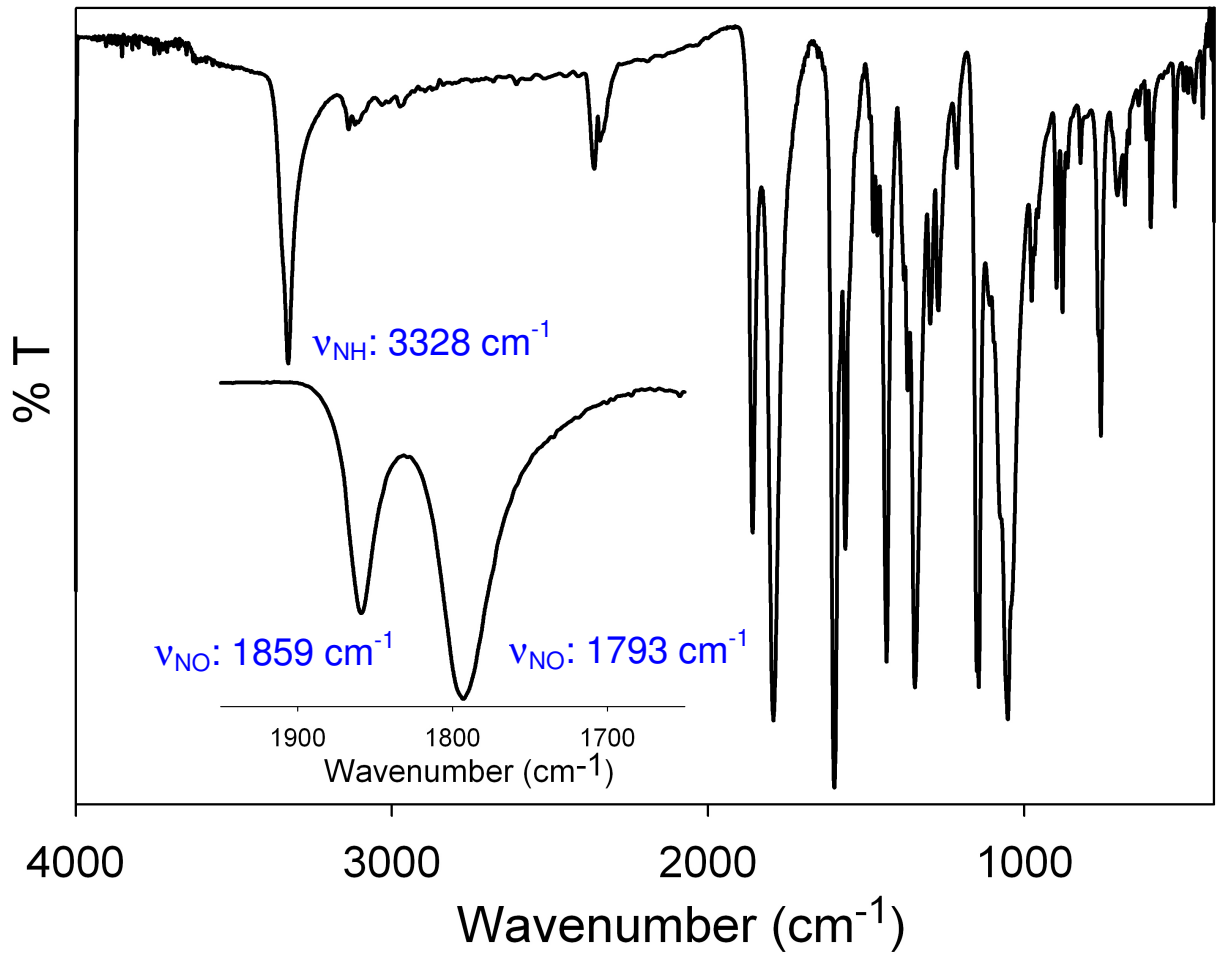

Figure S20. FTIR spectrum of $[Co(LN_4^{PhCl}H_2)(NO)_2]BF_4$ (**3**) in a KBr matrix. *Inset*: expansion of the N-O stretching (ν_{NO}) region.

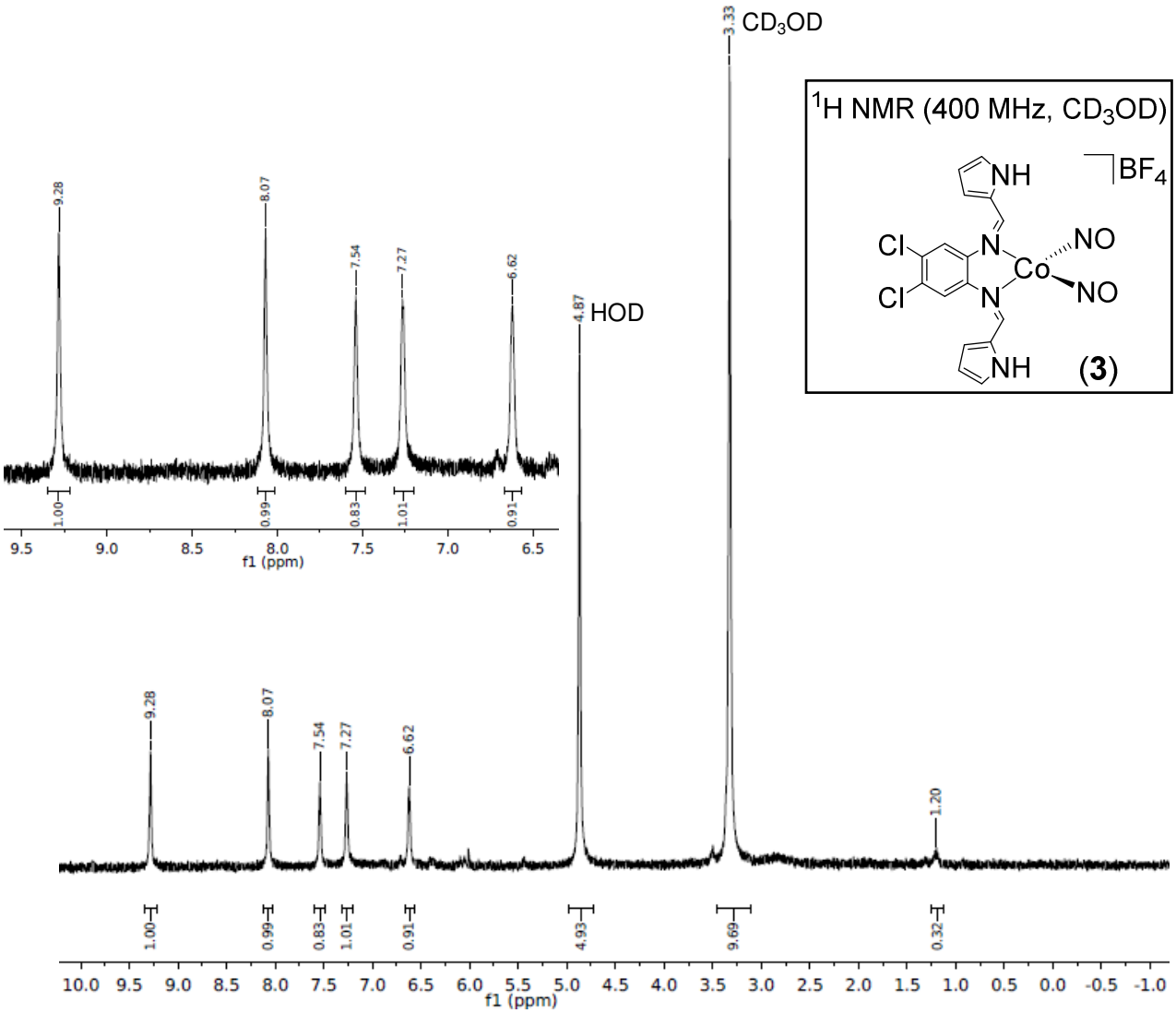

Figure S21. ^{1}H NMR spectrum of $[Co(LN_4^{PhCl}H_2)(NO)_2]BF_4$ (**3**) in CD_3OD at 298 K. The peaks at 3.33 and 4.87 are from residual protio solvent and H_2O, respectively. *Inset*: expansion of the aromatic region of the spectrum.

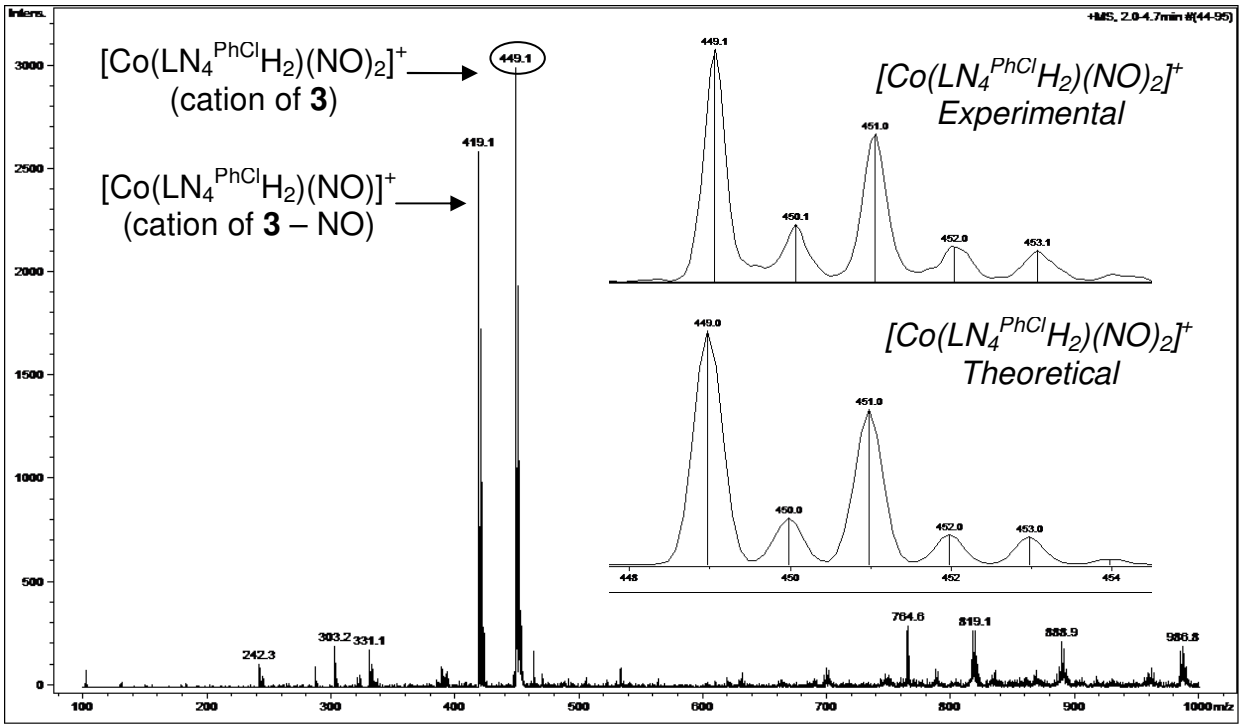

Figure S22. LR-ESI-MS (positive mode) of $[Co(LN_4^{PhCl}H_2)(NO)_2]BF_4$ (**3**) in MeOH. *Inset*: expansion of the molecular ion peak at *m/z*: 449.1 (top) and the theoretical fit (bottom).

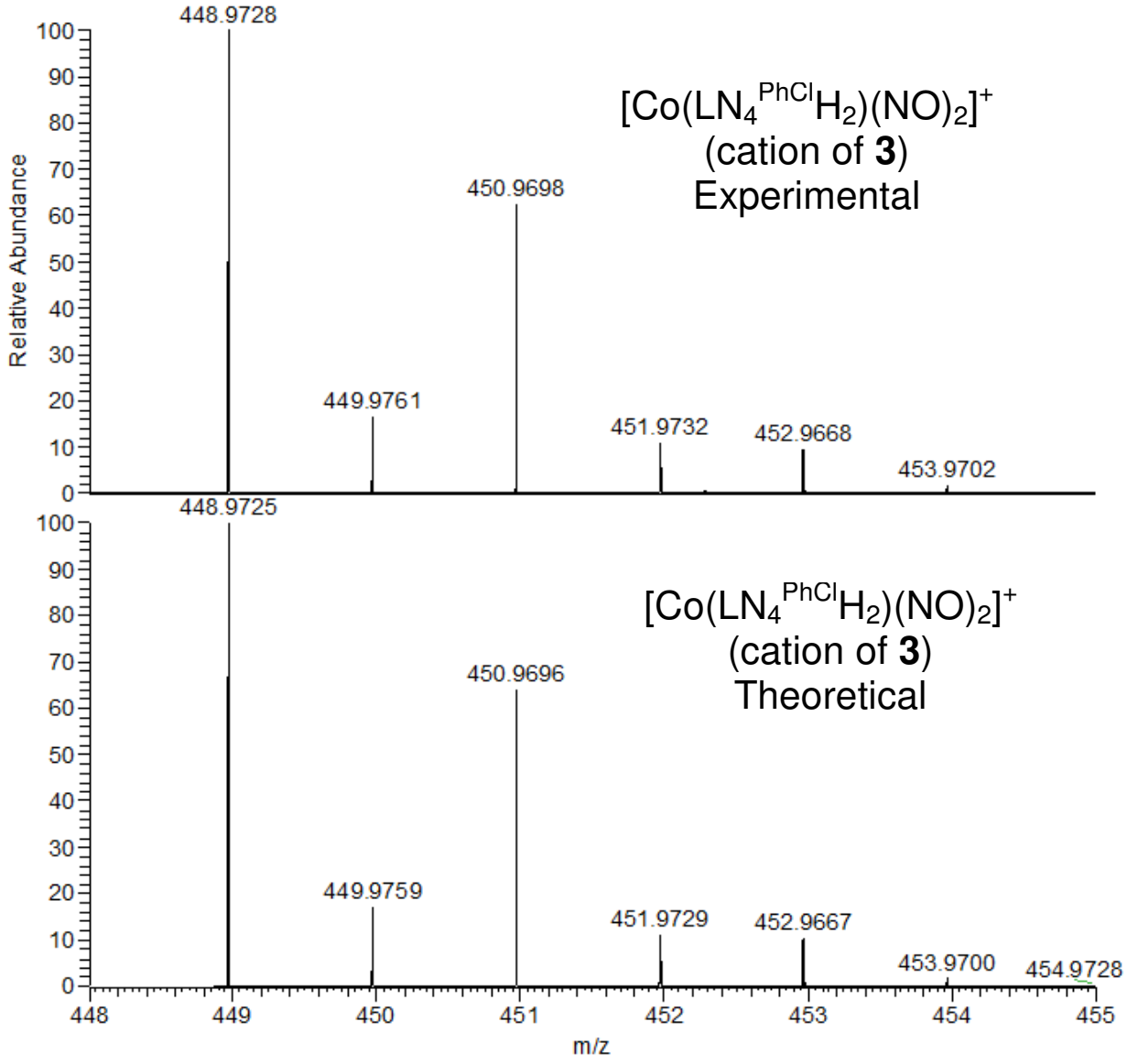

Figure S23. *Top*: High-resolution ESI-MS (positive mode) of $[Co(LN_4^{PhCl}H_2)(NO)_2]BF_4$ (**3**) in MeOH. *Bottom*: Theoretical MS for **3**.

References:

(1) Gill, N. S.; Taylor, F. B. *Inorg. Synth.* **1967,** *9*, 136.
(2) Sanders, B. C.; Patra, A. K.; Harrop, T. C. *J. Inorg. Biochem.* **2013,** *118*, 115.
(3) Sacco, A.; Rossi, M.; Nobile, C. F. *Ann. Chim. (Rome)* **1967,** *57*, 499.
(4) Fulmer, G. R.; Miller, A. J. M.; Sherden, N. H.; Gottlieb, H. E.; Nudelman, A.; Stoltz, B. M.; Bercaw, J. E.; Goldberg, K. I. *Organometallics* **2010,** *29*, 2176.
(5) (a) Armstrong, A.; Jones, L. H.; Knight, J. D.; Kelsey, R. D. *Org. Lett.* **2005,** *7*, 713; (b) Reisz, J. A.; Klorig, E. B.; Wright, M. W.; King, S. B. *Org. Lett.* **2009,** *11*, 2719.
(6) Cherryman, J. C.; Harris, R. K.; Davidson, M. G.; Price, R. D. *J. Braz. Chem. Soc.* **1999,** *10*, 287.
(7) Patra, A. K.; Afshar, R. K.; Rowland, J. M.; Olmstead, M. M.; Mascharak, P. K. *Angew. Chem. Int. Ed.* **2003,** *42*, 4517.
(8) Walker, F. A.; Lo, M.-W.; Ree, M. T. *J. Am. Chem. Soc.* **1976,** *98*, 5552.
(9) Reisz, J. A.; Zink, C. N.; King, S. B. *J. Am. Chem. Soc.* **2011,** *133*, 11675.
(10) (a) Trogler, W. C.; Marzilli, L. G. *Inorg. Chem.* **1974,** *13*, 1008; (b) Clarkson, S. G.; Basolo, F. *Inorg. Chem.* **1973,** *12*, 1528.
(11) Nakamoto, K., *Infrared and Raman Spectra of Inorganic and Coordination Compounds*. John Wiley & Sons: New York, 1986.
(12) *SMART v5.626: Software for the CCD Detector System*. Bruker AXS: Madison, WI, 2000.
(13) Walker, N.; Stuart, D. *Acta Crystallogr.* **1983,** *A39*, 158.
(14) Sheldrick, G. M. *SADABS, Area Detector Absorption Correction*, University of Göttingen: Göttingen, Germany, 2001.
(15) (a) Sheldrick, G. M. *SHELX-97, Program for Refinement of Crystal Structures*, University of Göttingen: Göttingen, Germany, 1997; (b) Sheldrick, G. M. *Acta Crystallogr.* **2008,** *A64*, 112.
(16) Sheldrick, G. M. *SHELXTL 6.1, Crystallographic Computing System*, Siemens Analytical X-Ray Instruments: Madison, WI, 2000.
(17) Cromer, D. T.; Waber, J. T., *International Tables for X-Ray Crystallography, Vol. IV, Table 2.2B*. The Kynoch Press: Birmingham, England, 1974.
(18) Burnett, M. N.; Johnson, C. K. *ORTEP-III, Report ORNL-6895*, Oak Ridge National Laboratory: Oak Ridge, TN, 1996.
(19) George, G. N.; George, S. J.; Pickering, I. J., EXAFSPAK, Stanford Synchrotron Radiation Lightsource, Menlo Park, CA. http://www-ssrl.slac.stanford.edu/~george/exafspak/exafs.htm. 2001.
(20) Cook, J. D.; Kondapalli, K. C.; Rawat, S.; Childs, W. C.; Murugesan, Y.; Dancis, A.; Stemmler, T. L. *Biochemistry* **2010,** *49*, 8756.
(21) Synergy Software, KaleidaGraph 4.1.3: [data analysis-graphing application: for Macintosh and Windows operating systems] http://www.synergy.com. 2011.
(22) Randall, C. R.; Shu, L.; Chiou, Y.-M.; Hagen, K. S.; Ito, M.; Kitajima, N.; Lachicotte, R. J.; Zang, Y.; Que Jr., L. *Inorg. Chem.* **1995,** *34*, 1036.
(23) Riggs-Gelasco, P. J.; Stemmler, T. L.; Penner-Hahn, J. E. *Coord. Chem. Rev.* **1995,** *144*, 245.